

Preventing Environmental Disasters from Grounding Accidents: A Case Study of Tugboat Positioning along the Norwegian Coast

Brice Assimizele^{a,d}, Johannes O Royset^b, Robin T. Bye^c, and Johan Oppen^d

^aFaculty of Maritime Technology and Operations, Norwegian University of Science and Technology, Ålesund, Norway

^bOperations Research Department, Naval Postgraduate School, Monterey, California, USA

^cFaculty of Engineering and Natural Sciences, Norwegian University of Science and Technology, Ålesund, Norway

^dDepartment of Logistics, Molde University College, Molde, Norway

Abstract

An important task of operators in Norwegian vessel traffic services (VTS) centers is to cleverly position tugboats before potential vessel distress calls. Here, we formulate a nonlinear binary-integer program, integrated in a receding horizon control algorithm, that minimizes the expected cost of grounding accidents by positioning tugboats optimally under uncertainty about vessel incidents and environmental conditions. Linearizations of the model lead to easy-to-compute bounds on the optimal value. Numerical experiments with real-world data demonstrate significant reduction in the expected cost, suggesting that the model can be used as a decision-support tool at VTS centers.

Keywords: OR in maritime industry; Mixed Integer Programming; Search and Rescue; Oil Spill

1 Introduction

During the last decades marine transportation of crude oil and petroleum products has increased considerably as well as its associated risk to the environment. Although accidental oil spills from tankers are relatively rare (Goerlandt and Montewka, 2014), oil transport remains one of the main concerns for various stakeholders in the protection of the marine environment (Dalton and Jin, 2010). Indeed, oil spills can result in severe consequences to the marine ecosystem (Lecklin et al., 2011). In addition, there are high socioeconomic costs, clean-up costs, and even possibility of loss of life. Most of the large oil spills are related to grounding and collision

accidents of oil tankers (Vanem et al., 2008). About one third of commercial ship accidents are caused by ship grounding accidents (ITOPF, 2013).

In Norway, several hundred oil tankers travel each year along the northern coastline. To monitor this traffic, the Norwegian Coastal Administration (NCA) operates a center for vessel traffic services (VTS) in the town of Vardø in northeastern Norway. The VTS center is responsible for the coastline from the Russian border in the Barents Sea to Rørvik near Trondheim, a distance of more than 600 nautical miles. The region is environmentally sensitive due to important fisheries and increasing tourism. About 200 vessels are monitored daily by the VTS center of which five to six oil tankers receive special attention due to their size or risk of pollution. These tankers are required by law to sail along a predefined corridor about 27 nautical miles from the coast. The VTS center operates a fleet of two tugboats with the purpose to intercept any vessel that lose steering, propulsion, or power, and drift towards land. Dynamic information (e.g., position, heading, speed over ground, rate of turn) and static information (e.g., identity, dimensions, cargo, flag) of the ships entering the region are obtained every two seconds on average through the Automatic Identification System (AIS). In addition to AIS information, weather forecast, real-time measurements of ocean currents, wave height, and wind are available to predict drift trajectories. At any time, an oil tanker moving in the region may lose its maneuverability, e.g., through steering or propulsion failure. Thus, the tugboats have to be sufficiently close to hook-up with any drifting oil tanker before it runs ashore.

The increasing oil tanker traffic in the High North makes it difficult for the VTS operators to dynamically position the tugboats to locations where they can be the most effective. In an effort to improve the positioning of tugboats, the authors were invited by the NCA to visit the VTS center in Vardø and suggest improvements in the process. This paper reports models for the optimal tugboat positioning (OTP) problem as well as computational results obtained after the visit and subsequent meetings and exchanges of information with the VTS center and the NCA representatives. NCA is currently evaluating the possibility to implement the models in a decision support system operating at the VTS. This paper is the first to formulate the OTP problem and demonstrate the benefits from its solution using historical events.

The remainder of the paper is organized as follows. In Section 2, we introduce the related literature on emergency response and safety organization. In Section 3, formulate a nonlinear binary integer program (BIP) for the OTP problem with two linearizations. Section 4 gives methods for obtaining input data to the models, and Section 5 presents computational experiments. The paper ends with conclusions and a discussion of further research in Section 6.

2 Related Literature

We present a review on general resource location/allocation and patrol routing problems, where safety organization and emergency response systems are the primary concern, followed by specific literature on the OTP problem.

General models on resource allocation and patrol routing problems in the literature include p -median problems (p -MP) (Campbell, 1996; Church and ReVelle, 1976; Church et al., 2004; Ishfaq and Sox, 2010), p -center problems (p -CP) (Davidović et al., 2011; Drezner, 1984; Espejo et al., 2015; Suzuki and Drezner, 1996), covering problems that are categorized into maximal covering location problems (MCLP) (Balcik and Beamon, 2008; Church and ReVelle, 1974; Davari et al., 2011), set covering problems (SCP) (Badri et al., 1998; Beasley and Jørnsten, 1992; Caprara et al., 2000), maximum coverage patrol routing problems (MCPRP) (Capar et al., 2015; Dewil et al., 2015; Keskin et al., 2012; Li and Keskin, 2013) and police districting problems (PDP) (Camacho-Collados and Liberatore, 2015; D'Amico et al., 2002).

The OTP problem closely relates to maritime search and rescue (SAR) operations. SAR operations consist of search for missing or distressed vessels followed by their rescue. Basdemir (2004) proposes an MCLP that allocates SAR helicopters to candidate bases to satisfy predefined incidents regions. A combination of p -MP and p -CP models are used in Dawson et al. (2007) to determine the locations of security teams over a geographic area to maintain security for the United States air force intercontinental ballistic missile systems. The combined model minimizes both the distance traveled and the maximum distance from any missile site to required security forces. An optimization and simulation method is used in Afshartous et al. (2009) to determine the locations of the United States coast guard air stations to respond to emergency distress calls. They model the problem as a p -Uncapacitated Facility Location Problem (p -UFLP). The authors assume the demand for each client to be equal and served with a single resource. A similar problem is presented in Razi and Karatas (2016), but the demand for each incident varies and each demand can be covered from multiple resources. Radovilsky and Koermer (2007) develop an integer linear programming model to optimally allocate small boats to the United States coast guard (USCG) stations. Their objective function minimizes the shortage or excess capacity at the stations. An improved formulation called boat allocation tool (BAT) is developed by Wagner and Radovilsky (2012), but do not consider actual locations of incidents and the corresponding response time. Chircop et al. (2013) address the fleet sizing problem faced by the Royal Australian Navy (RAN) with a column generation algorithm incorporated into a branch-and-price framework. A fleet patrol boats should be able to provide complete coverage of a set of specified patrol regions. Moreover, Millar and Russell (2012) develop a binary integer programming model (BIP) for the fisheries surveillance patrol routing problem in the Canadian Atlantic offshore groundfish fishery. The primary goal of the fisheries patrol routing problem is to maximize the deterrent effect of a patrol vessel through routing over a network of fishing grounds. They are the first to formulate this problem, which relates to the selective traveling salesman problem, where the fishing grounds represent the cities, and all or a subset of grounds is visited on a given trip. Their model, however, focuses more on scheduling than boat positioning. Pelot et al. (2015) categorize SAR boats based on their capabilities and use historical incident data to solve the allocation problem for the Canadian coast guard. In their study, incidents are classified based on their severity and a response time requirement

is established for each type. Similarly, Eide et al. (2007) develop a dynamic risk model that prioritize oil tankers based on their potential oil spill volume in case of grounding accidents and subdivide the northern Norwegian coastline in segments, where each segment has an associated risk level. The model estimates the environmental risk of a drift grounding accident occurring with a specific tanker, at a given location, and under current weather conditions. Drift trajectories with high risk can then be prioritized in the planning of tugboat positions. Abi-Zeid and Frost (2005) develop a geographic decision support tool (SRAPlan) based on search theory to assist the Canadian forces in the planning of search missions for missing aircrafts. A similar system is also developed for the Polish SAR teams (Wysokiński et al., 2014).

All these tools and models, despite their importance, do not suggest how and where the fleet of tugboats should move in order to minimize risk. Razi and Karatas (2016) on the other hand develop a tactical model for determining the optimal placement of SAR boats, however their model do not account for uncertainty related to vessel incidents and the dynamic nature of the SAR resources positioning, which are the primary concern of the OTP problem. To determine the optimal positions of tugboats in real time, researchers have developed methods both including genetic algorithms (Bye, 2012; Bye and Schaathun, 2014, 2015a,b) and an MIP model (Assimizele et al., 2013). Their algorithms and models assume oil tankers move along piecewise-linear corridors and approximately parallel to the coastline. Additionally, their proposed set of objective functions focuses mainly on the minimization of distances between future tugboat positions and locations where hook-up with a drifting vessel might be possible. However, in situations with multiple tugboats, sum of distances are not effective surrogates for the probability of successful hook-up between a tugboat and a vessel and the cost associated with failure to do so. In addition, a distance minimization will not capture the different consequences associated with each vessel type and grounding location. Moreover, a one-dimensional modeling approach also has less flexibility in geographical positioning. All these weaknesses are addressed in this paper with a two-dimensional nonlinear binary integer programming model.

In contrast to the optimization of SAR and related operations (see for example Alpern and Gal (2002); Pietz and Royset (2014); Royset and Sato (2010); Shechter et al. (2015); Stone et al. (2016) and references therein), where search for a vessel is a central aspect, operators in the present context know the location of vessels. In an OTP problem, a tanker in distress has a known current location due to the continuously transmitted AIS information. That is, the OTP problem is primarily a rescue mission. However, uncertainty about which vessel will need assistance and the subsequent drift trajectories and weather conditions add complexity to the process of planning current and future tugboat positions. Thus, our aim is to assist the VTS operators by developing a nonlinear BIP model integrated in a receding horizon control algorithm that minimizes the expected environmental cost associated with grounding vessels and utilizes a two-dimensional discretization of the coastal zone. Royset and Sato (2010) adopt a similar two-dimensional modeling approach by subdividing the region of interest into a finite set of cells in a discrete-time route-optimization problem, where searchers seek to detect randomly

moving targets.

3 Model Formulation

We subdivide the High North region controlled by the VTS center in Vardø into a finite number of cells $\mathcal{C} = \{1, \dots, C\}$ and discretize the planning horizon into a finite set of time periods $\mathcal{T} = \{0, 1, \dots, T\}$. Each vessel (oil tanker) in the set $\mathcal{V} = \{1, \dots, V\}$ occupies one cell at each time period and can move to any reachable cell in a time period depending on its speed, which is influenced by the weather conditions.

Every vessel $v \in \mathcal{V}$ is associated with a family of possible paths and times when it might become in distress. A path $p = (c_1, c_2, \dots, c_T)$, $c_t \in \mathcal{C}$, is a sequence of cells representing the trajectory of the vessel over time. The pair $\omega_v = (t, p)$ gives a vessel scenario for vessel v , where p is the associated path and $t \in \mathcal{T} \cup \{T + 1\}$ is the time the VTS center is alerted to the distress of vessel v . Typically, the vessel reports steering failure, loss of propulsion, and other issues through AIS. However, sometimes incidents go unreported and the VTS center might simply observe a change in heading and speed. We let Ω_v be the set of scenarios for vessel v . Typically, each vessel has a scenario (t, p) where the path p is the planned trajectory of the vessel in the absence of failure. In this case, there will be no distress call and the time t is set to $T + 1$. In addition, we define $\bar{\omega} = (\omega_1, \dots, \omega_V) \in \bar{\Omega}$, where $\bar{\Omega} = \Omega_1 \times \dots \times \Omega_V$ is the collection of all scenarios.

Let $\mathcal{G} = \{1, \dots, G\}$ be the set of tugboats operated by the VTS center in Vardø. At the beginning of the planning horizon, each tugboat $g \in \mathcal{G}$ is positioned at cell $c_{0g} \in \mathcal{C}$. The tugboats can transit between reachable cells each time period. Specifically, let $\mathcal{F}_{tg}(c) \subset \mathcal{C}$ be the set of cells that are adjacent to $c \in \mathcal{C}$ in period t for tugboat g . That is, the set of cells reachable from cell c in one time period by tugboat g . The set $\mathcal{F}_{tg}(c)$ depends on the weather conditions in time period t and the maximum speed for tugboat g . Additionally, the fleet of tugboats are not allowed to move far away from the coastline because of a secondary escort mission; some of the ships in transit to ports located in the north of Norway need to be escorted by tugboats. This secondary task does not influence the model we develop as the available number of tugboats at each time period in the planning horizon is known well in advance.

A vessel might start drifting at any time period with a certain probability, which depends on internal factors of the vessel as well as the weather conditions (e.g., ocean current, wave height). Moreover, the path followed while drifting is also determined by environmental factors. In Section 4, we give details about how the specifics of a scenario can be computed. We let R_{ω_v} be the probability of scenario ω_v for vessel v . We assume that the probabilities of failure through steering or propulsion are independent between vessels. Although this assumption might not always be reasonable, here we justify it by the fact that vessels in distress are usually spatially separated with few common environmental factors. Hence, the probability for a scenario $\bar{\omega}$ is given by $R_{\bar{\omega}} = \prod_{v \in \mathcal{V}} R_{\omega_v}$. A critical component is a tugboat's ability to hook-up with a vessel

that is drifting next to it. We let the probability of successful hook-up by tugboat g with vessel v , given vessel v follows scenario $\omega_v = (t, p)$ and tugboat g is in cell c at time of distress call t , be denoted by $Q_{gc\omega_v}$.

The aim is to move tugboats between cells in such a way that the expected cost of ship grounding accidents is minimized. Let K_{ω_v} be the grounding cost associated with vessel scenario $\omega_v = (t, p)$, i.e., the cost for a vessel following path p and no tugboat manages to hook-up with the drifting vessel. We note that K_{ω_v} is a deterministic quantity, but it is trivial to account for uncertainty in the cost by defining additional vessel scenarios. The cost mostly depends on the grounding location as well as the type and volume of the oil spill. This cost is equal to zero for vessel scenarios having $t = T + 1$, i.e., no failure occurs and the vessel follows a normal route in the corridor. We define x_{gct} as a binary variable that takes the value 1 if tugboat g is in cell c at time t , and 0 otherwise. For a tugboat g in cell c at time of distress t , the probability of not being able to hook-up with vessel v following scenario $\omega_v = (t, p)$ is $1 - Q_{gc\omega_v}$. Thus, the probability that no tugboat rescues vessel v if vessel scenario ω_v occurs equals

$$\prod_{g \in \mathcal{G}, c \in \mathcal{C}} (1 - Q_{gc\omega_v})^{x_{gct}}.$$

Note that subscript t in the variable x_{gct} is the time of distress in scenario $\omega_v = (t, p)$ and the probability of hook-up $Q_{gc\omega_v}$ is relative to that time. Then, the expected grounding cost for scenario $\bar{\omega}$ equal

$$\sum_{v \in \mathcal{V}} K_{\omega_v} \prod_{g \in \mathcal{G}, c \in \mathcal{C}} (1 - Q_{gc\omega_v})^{x_{gct}}. \quad (1)$$

The expected total cost across all scenarios follows as

$$\sum_{\bar{\omega} = (\omega_1, \dots, \omega_V) \in \bar{\Omega}} R_{\bar{\omega}} \sum_{v \in \mathcal{V}} K_{\omega_v} \prod_{g \in \mathcal{G}, c \in \mathcal{C}} (1 - Q_{gc\omega_v})^{x_{gct}}, \quad (2)$$

which we denote by $f(\mathbf{x})$, where \mathbf{x} is the vector with components x_{gct} . Let $\alpha_{gc\omega_v} = -\ln(1 - Q_{gc\omega_v})$ be the *hook-up rate*. The function f can be equivalently written as:

$$f(\mathbf{x}) = \sum_{\bar{\omega} = (\omega_1, \dots, \omega_V) \in \bar{\Omega}} R_{\bar{\omega}} \sum_{v \in \mathcal{V}} K_{\omega_v} \exp \left(- \sum_{g \in \mathcal{G}} \sum_{c \in \mathcal{C}} \alpha_{gc\omega_v} x_{gct} \right). \quad (3)$$

Since costs are nonnegative, f is a convex function. In fact, the exponential function is convex and f is a sum of exponential functions. In the following subsections, we formulate the OTP problem as a nonlinear BIP and give linear approximations.

3.1 OTP Model

A nonlinear BIP model is developed next to minimize the objective function f in (3) subject to operational constraints.

OTP model:

Indices

t	time period
c, c', c_t	cells
v	vessel
g	tugboat
p	path $p = (c_1, \dots, c_T)$
ω_v	scenario for vessel v ; $\omega_v = (t, p)$
$\bar{\omega}$	scenario for all vessels $\bar{\omega} = (\omega_1, \dots, \omega_V)$

Sets

C	set of cells $C = \{1, \dots, C\}$
$\mathcal{F}_{tg}(c) \subseteq C$	set of cells reachable from cell c in period t for tugboat g
\mathcal{V}	set of vessels $\mathcal{V} = \{1, \dots, V\}$
\mathcal{G}	set of tugboats $\mathcal{G} = \{1, \dots, G\}$
\mathcal{T}	set of time periods $\mathcal{T} = \{0, 1, \dots, T\}$
Ω_v	set of scenarios for vessel v
$\bar{\Omega}$	set of all possible scenarios $\bar{\Omega} = \Omega_1 \times \dots \times \Omega_V$

Parameters

K_{ω_v}	grounding cost for vessel v in scenario $\omega_v = (t, p)$
R_{ω_v}	probability for vessel scenario $\omega_v = (t, p)$
$R_{\bar{\omega}}$	probability for scenario $\bar{\omega} = (\omega_1, \dots, \omega_V)$, $R_{\bar{\omega}} = \prod_{v \in \mathcal{V}} R_{\omega_v}$
$Q_{gc\omega_v}$	probability of successful hook-up by tugboat g with vessel v , given tugboat g is in cell c at time of distress call t and vessel v follows scenario $\omega_v = (t, p)$
$\alpha_{gc\omega_v}$	hook-up rate with vessel v for tugboat g in cell c under scenario ω_v , $\alpha_{gc\omega_v} = -\ln(1 - Q_{gc\omega_v})$

Variables

x_{gct}	binary variable taking the value 1 if tugboat g is in cell c at time t , 0 otherwise
-----------	--

Formulation

$$\min f(\mathbf{x})$$

s.t.

$$\sum_{c \in \mathcal{F}_{ig}(c')} x_{gct-1} \geq x_{gc't} \quad \forall g \in \mathcal{G}, \forall c' \in \mathcal{C}, \forall t \in \mathcal{T} \setminus \{0\} \quad (4)$$

$$\sum_{c \in \mathcal{C}} x_{gct} = 1 \quad \forall g \in \mathcal{G}, \forall t \in \mathcal{T} \quad (5)$$

$$x_{g,c_{0g},0} = 1 \quad \forall g \in \mathcal{G} \quad (6)$$

$$x_{gct} \in \{0, 1\} \quad \forall g \in \mathcal{G}, \forall c \in \mathcal{C}, \forall t \in \mathcal{T} \quad (7)$$

Constraints (4) ensure tugboats move only between reachable cells. In addition, constraints (5) make sure tugboats are not located in more than one cell in any time period. Constraints (6) give initial positions of tugboats. That is, cell c_{0g} is the position of tugboat g at the beginning of the planning horizon.

3.2 Linearization of the Objective Function

Since a direct solution of the OTP model might be computationally costly, we develop two approaches to linearize the objective function f and obtain two resulting mixed-integer linear programming models MIP-L and MIP-U. A viable alternative could be the continuous relaxation (Branch-and-bound) to the convex problem using standard mixed-integer nonlinear program (MINLP) solvers. However, Royset and Sato, (2010) use a similar nonlinear convex exponential function to address the discrete-time route-optimization problem. They present two solutions approaches, one based on the cutting-plane (linearization) method and the other on continuous relaxation of the objective function. The cutting-plane approach, compared with the existing branch-and-bound algorithm (fail to find solutions), is able to solve many realistically sized problems instances in few minutes. Their specialized cut improves the solution time by about 50% and further reduce the solution time with about two orders of magnitude. In their study, standard MINLP solvers, Bonmin and DICOPT, have higher solution time compared to CPLEX with the linearized model. Moreover, the effective cut-building technology in mixed-integer linear program (MIP) are not available in the MINLP solvers.

3.2.1 Lower Linearization: MIP-L

New nonnegative variables z_{ω_v} are included to remove the nonlinearity in the objective function through the standard lower-bounding approximation (Ramos, 2007; Royset and Sato, 2010)

$$\exp(-y) \geq \max_{k \in \mathcal{K}} \{ \exp(-y_k) - \exp(-y_k)(y - y_k) \} \quad \forall y, y_k \in \mathbb{R}, k \in \mathcal{K}.$$

Accordingly, let $Y_{\omega_v, k} \in \mathbb{R}$, $k \in \mathcal{K}$, where \mathcal{K} represents the set of breakpoints. The resulting mixed-integer linear model (MIP-L) takes the following form.

Model MIP-L:

Additional Set

\mathcal{K} set of breakpoints $\mathcal{K} = \{1, \dots, K\}$

Additional Parameters

$Y_{\omega_v, k}$ breakpoint number $k, k \in \mathcal{K}$ for vessel scenario ω_v

Additional Variables

z_{ω_v} nonnegative variable used for linearization
for vessel scenario ω_v

Formulation

$$\min \sum_{\tilde{\omega}=(\omega_1, \dots, \omega_V) \in \tilde{\Omega}} R_{\tilde{\omega}} \sum_{v \in \mathcal{V}} K_{\omega_v} z_{\omega_v}$$

s.t.

(4)-(7) and

$$\exp(-Y_{\omega_v, k}) - \exp(-Y_{\omega_v, k}) \left(\sum_{g \in \mathcal{G}} \sum_{c \in \mathcal{C}} \alpha_{gc\omega_v} x_{gct} - Y_{\omega_v, k} \right) \leq z_{\omega_v}, \forall \omega_v = (t, p) \in \Omega_v, \forall v \in \mathcal{V}, \forall k \in \mathcal{K}$$

$$z_{\omega_v} \geq 0 \quad \forall \omega_v = (t, p) \in \Omega_v, \forall v \in \mathcal{V}$$

Let θ_{OPT} and $\theta_{\text{MIP-L}}$ be the optimal value for the OTP and MIP-L models, respectively. Obviously, $\theta_{\text{MIP-L}} \leq \theta_{\text{OPT}}$.

3.2.2 Upper Linearization: MIP-U

It is well known (Bazaraa et al., 1995; Lin et al., 2013) that $\exp(-y)$ can be bounded from above on $[0, y_{\max}]$ by a piecewise linear function that coincides with $\exp(-y_k)$ at points $y_k \in [0, y_{\max}]$, $k \in \mathcal{K}$. We apply this approach to the term $\exp(-\sum_{g \in \mathcal{G}} \sum_{c \in \mathcal{C}} \alpha_{gc\omega_v} x_{gct})$ and set $y_{\max} = \sum_{g \in \mathcal{G}} \max_{c, \omega_v} \alpha_{gc\omega_v}$. The piecewise linear function is most easily represented by nonnegative auxiliary variables that sums to one. Specifically, $\sum_{k \in \mathcal{K}} \lambda_k \exp(-y_k) \geq \exp(-\sum_{k \in \mathcal{K}} \lambda_k y_k)$ for $0 \leq \sum_{k \in \mathcal{K}} \lambda_k y_k \leq y_{\max}$. Using these relations, we obtain the upper-bounding model MIP-U as follows:

Model MIP-U:

Additional Parameters

$Y_{\omega,k}, F_{\omega,k} = \exp(-Y_{\omega,k})$ function values at $k \in \mathcal{K}$

Additional Variables

$\lambda_{\omega,k}$ nonnegative variable used for linearization

Formulation

$$\min \sum_{\bar{\omega}=(\omega_1, \dots, \omega_V) \in \bar{\Omega}} R_{\bar{\omega}} \sum_{v \in \mathcal{V}} K_{\omega_v} \left(\sum_{k \in \mathcal{K}} \lambda_{\omega_v,k} F_{\omega_v,k} \right)$$

s.t.

(4)-(7) and

$$\begin{aligned} \sum_{g \in \mathcal{G}} \sum_{c \in \mathcal{C}} \alpha_{gc\omega_v} x_{gct} &= \sum_{k \in \mathcal{K}} \lambda_{\omega_v,k} Y_{\omega_v,k} \quad \forall \omega_v = (t, p) \in \Omega_v, \forall v \in \mathcal{V} \\ \sum_{k=1}^K \lambda_{\omega_v,k} &= 1 \quad \forall \omega_v = (t, p) \in \Omega_v, \forall v \in \mathcal{V} \\ \lambda_{\omega_v,k} &\geq 0 \quad \forall \omega_v \in \Omega_v, \forall v \in \mathcal{V}, \forall k \in \mathcal{K} \end{aligned}$$

The optimal value of MIP-U provides an upper bound for θ_{OPT} . However, it is obviously better to use the true objective function value. Accordingly,

$$\theta_{\text{MIP-L}} \leq \theta_{\text{OPT}} \leq \min\{f(\bar{\mathbf{x}}), f(\underline{\mathbf{x}})\},$$

where $\bar{\mathbf{x}}$ and $\underline{\mathbf{x}}$ are the vectors of optimal x_{gct} for MIP-U and MIP-L, respectively. We observe that MIP-L suffices to generate both upper and lower bounds on θ_{OPT} , but we also include MIP-U as it solves much faster than MIP-L and sometimes yields better solutions.

4 Input Parameters

In this section, we present preliminary methods to obtain accurate input parameter to the OTP model

4.1 Hook-up Probabilities

Each drifting vessel is detected by the VTS center, which in turn informs the nearest tugboat. The time needed for a tugboat to reach the drifting vessel depends on the reaction and mobilization time, sailing time from the initial tugboat position to the vessel and the time required to hook-up the vessel to the tugboat. It takes on average 2 hours to hook-up the drifting vessel with

the tugboat when they are next to each other, but this can increase in bad weather conditions (Eide et al., 2007). Once the vessel is reached by the tugboat, the time, t_l , left before it runs ashore will determine the probability of successful hook-up. Recall that $Q_{gc\omega_v}$ is the probability of successful hook-up by tugboat g to vessel v , given tugboat g is in cell c at time t and vessel v follows $\omega_v = (t, p)$. For every vessel scenario and tugboat position, we determine t_l using the maximum speed of the tugboat and the location of c relative to p , and set

$$Q_{gc\omega_v} = \frac{\beta_{\omega_v} \exp(\delta_{\omega_v}(t_l - t_{\min}))}{1 + \exp(\delta_{\omega_v}(t_l - t_{\min}))}.$$

The parameter t_{\min} represents the minimal remaining drift time required to attempt hook-up. If t_l is less than t_{\min} , $Q_{gc\omega_v}$ is set to 0. In addition, $\beta_{\omega_v} \in [0, 1]$ and $\delta_{\omega_v} \geq 0$ represent the influence of weather. This model is a preliminary attempt to estimate the hook-up probabilities. Further work is needed to fit the model using empirical data from field tests and actual accidents, which is nontrivial work and beyond the scope of the paper. Nevertheless, we have included the weather and current factors in the experiments with real-world data. In fact, the maximal operational speeds of the tugboats at each cells depend on the current and wind forces as well as wave height. Moreover, the formula simply transform the time left t_l , into a value between zero and one. In addition, for every time left t_{l_1} and t_{l_2} , we have the following condition: If $t_{l_1} \leq t_{l_2}$ then $Q_{gc\omega_v}(t_{l_1}) \leq Q_{gc\omega_v}(t_{l_2})$, which is a necessary and sufficient condition to optimally move tugboats in cells with higher response time.

4.2 Drift Trajectories

The motion of a drifting vessel is entirely determined by the sum of surface and body forces acting on it (Jankowski, 1992). The forces acting on the surface are caused by the buoyancy force, the sea surface current, surface wind and the waves. The gravitational force is the only body force acting on its center of mass.

The drift caused by the wind alone is termed the object's *leeway* (Hodgins and Mak, 1995). Because of the asymmetric shape of the vessel, the drag and lift component of the wind will cause the object to drift at an angle relative to the wind called "leeway angle". The Norwegian Meteorological Institute (NMI) developed a LEEWAY model as part of its oceanic trajectory models suite for Search and Rescue, Vessel Traffic Service and Environmental Protection Agency (Breivik and Allen, 2008).

Uncertainty parameters such as leeway divergence angle is obtained through Monte Carlo simulation (Breivik and Allen, 2008) and field investigation (Allen and Plourde, 1999). Ni et al. (2010) present a theoretical drift prediction based on the law of physics and non-probabilistic analysis of uncertainty. Consider a vessel in steady drift with velocity U_B subjected to a forcing field with constant wind velocity U_W and a constant current velocity U_C . The law of motion dictates that the relative wind force $U_W - U_B$ and the leeway force $U_B - U_C$ must be opposite to each other. In addition, the sum of the two forces are equal to zero for a steady drift. Thus, the

drift velocity can be expressed as follow:

$$U_B = \frac{1}{1+\tau}U_C + \frac{\tau}{1+\tau}U_W = U_C + \mu(U_W - U_C),$$

where μ is the leeway rate and $\tau^2 = (C_D A \rho)_1 / (C_D A \rho)_2$. The subscripts 1 and 2 refer to the in-air and in-water quantities respectively, where C_D is the drag coefficient, A is the cross-sectional area exposed, and ρ is the fluid density. More details can be found in Ni et al. (2010). This formula does not consider the wave drift force which can be expressed by $F = \frac{1}{2}\rho_2 f_g L C_{2W} a^2$. The wave amplitude is one-half of the wave height and is represented by a , C_{2W} denotes the wave drift coefficient and L is the vessel length and f_g is the gravitational force. Hence, the drift velocity with wave force included can be expressed as follow:

$$U_B = \tilde{U}_B - \frac{\tilde{U}_B - U_C}{1 - \tau} + \sqrt{\left(\frac{\tilde{U}_B - U_C}{1 - \tau}\right)^2 + \frac{\chi}{1 - \tau^2}}, \quad (8)$$

where \tilde{U}_B is the solution of the equation of motion in the absence of waves and the parameter

$$\chi = \frac{f_g L C_{2W} a^2}{(C_D A)_2}.$$

As the region is discretized into cells, it is possible to estimate, for every time period, the next position of a drifting vessel given information on the local wind, surface current of the initial position, and the shape and buoyancy of the vessel. For every vessel and time step, we can estimate a potential drift trajectory using (8), which is represented by a sequence of cells (see Figure 1). Specifically, we compute a path for a vessel as follows.

Step 0:

Set $i := 0$ and $p := (c_t)$, where c_t represents the position of the vessel at the time of distress call $t \leq T$.

Step 1:

Obtain the wind, current velocities and wave force as well as actual vessel velocity from the AIS for the current cell c_{t+i} and set $i := i + 1$.

Step 2:

Determine the new actual vessel velocity, U_B , using the formula in (8) as illustrated in Figure 1.

Step 3:

Determine in which cell falls the new obtained vessel force U_B and denote it by c_{t+i} ; and set $p := (c_t, \dots, c_{t+i})$.

Step 4:

Go back to Step 1 or stop if the current cell c_{t+i} is ashore or outside the region of interest.

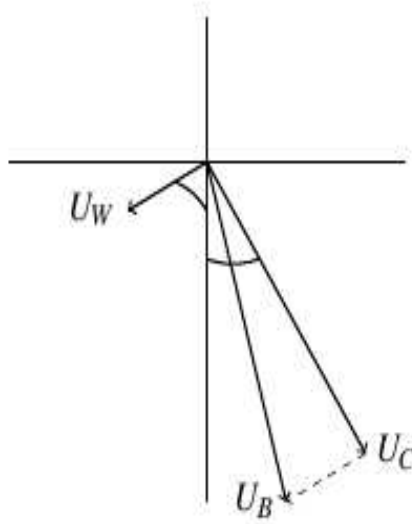


Figure 1: Drift velocity

The algorithm above does not generate the whole path followed by the vessel, but only from the time of distress call at cell c_i to shore. However, it is trivial to include the other parts of the path.

4.3 Environmental Costs and Drift Probabilities

Vessel grounding accidents can result in severe pollution from oil spills and damage to the environment. In addition, the oil spill highly depend on vessel type (Talley et al., 2012), capacity and grounding location. These consequences can be evaluated in terms of costs for a better classification of vessels and potential grounding locations.

About 34% of oil spills in European seas are caused by vessel grounding accidents (see Figure 2). One of the best known grounding-related oil spill accident is that of the Sea Empress in 1996, which ran aground in the entrance to Milford Haven, in the southwestern United Kingdom. The vessel released a total of 72,360 tonnes of oil into the sea (ITOPF, 2013).

The main factors influencing the cost of oil spills include the type of oil, amount of oil spilled and spillage rate, the physical, biological and economic characteristics of the spill location, and the weather and sea conditions at the time of the spill (Grey, 1999; Kontovas et al., 2010; Vanem et al., 2008; White and Molloy, 2003). The levels and types of cleanup capabilities to optimally respond to oil spills are outside of the scope of this paper (see Psaraftis et al. (1986) for related research in this area). Although a grounding vessel might not lose its entire cargo, the vessel size indicates the potential volume of oil spill. In addition, the amount of oil spill depends on the grounding location. A vessel running aground on hard rock will likely cause more oil spills than grounding on sand.

Vanem et al. (2008) develop a model that incorporates all costs of oil tanker spill accidents. They consider the spill amount as the major factor with a global average cleanup cost

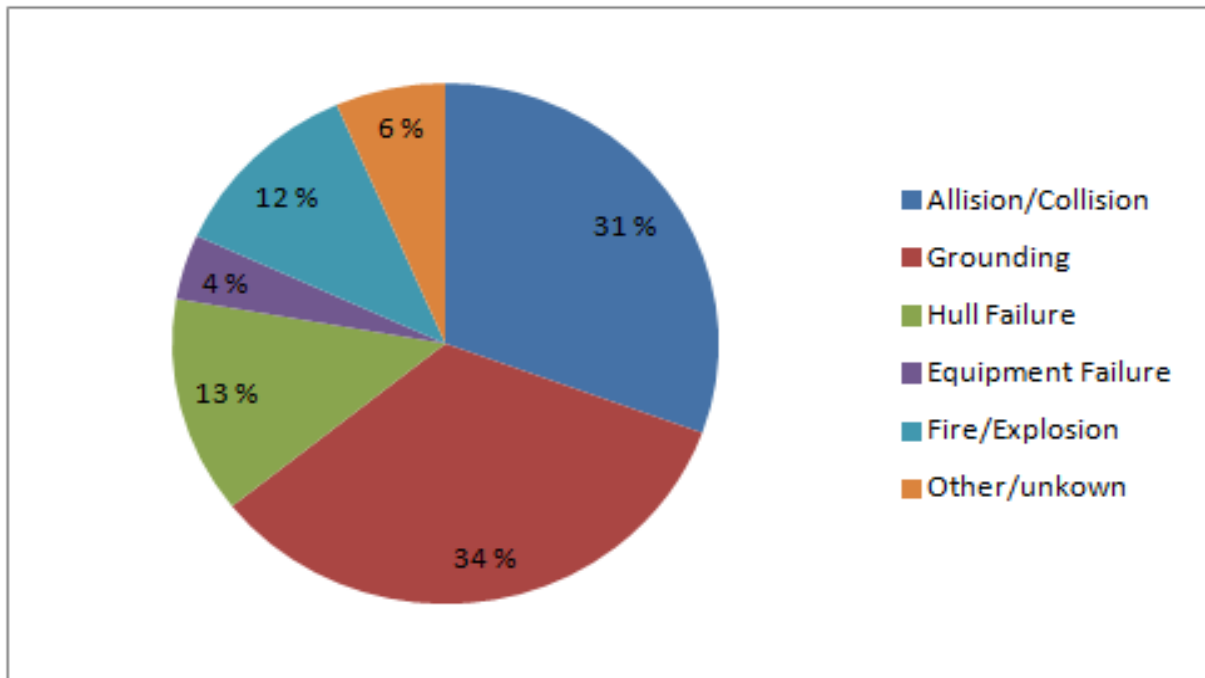


Figure 2: Volume of oil spilled per cause of accidents in European Seas for accidents above 7 tonnes per spill (Data Source: ITOPF 2013)

of USD 16,000/tonne. In addition to the cleanup cost, average environmental damage and socioeconomic costs are estimated to be around USD 24000/tonne. Research conducted about Norwegian waters assesses the environmental damage to be almost twice the cost associated with cleanup and rescue operations (Viggo, 2003). Kontovas et al. (2010) use a regression analysis of oil spill cost with data from the IOPCF (International Oil Pollution Compensation Federation) and obtain a total cost $K = 51.432V^{0.728}$ in terms of V , the volume in tonne of oil spilled. The total cost, in USD, includes three cost categories: cleanup, socioeconomic losses and environmental costs. In this paper, the cost related to each vessel scenario in the OTP model are obtained from this total cost formula with V determined by the size of the vessel and the part of the coast it might hit as categorized by Eide et al. (2007).

In the model formulation, R_{ω_v} , with $\omega_v = (t, p)$, is the probability for vessel v to start drifting along the path p at time $t \in \mathcal{T}$. The probability mainly depends on human factors (experience of nautical officers, excessive fatigue, stress and usage of alcohol), type of vessel (size, wind exposure area of the ship, flag state, age of the vessel), weather conditions, and the characteristics of the route (length, depth and width of the waterway). Sophisticated methods, such as fault tree analysis (Kum and Sahin, 2015; Mokhtari et al., 2011; Senol et al., 2015), for determining R_{ω_v} are beyond the scope of this paper. We simply generate these probabilities randomly in the simulation experiments, based on historical information both about how often drifts actually occur on average, and also about how much the probabilities vary between vessels due to different characteristics, such as flag state, age, and previous incidents.

5 Case Studies

In this section, we discuss the effectiveness, efficiency and performance of the models through three different case studies. First, we present the general settings common to all cases. Second, an illustrative example of the model and output is presented in Case 1. Third, we compare the MIP-L and MIP-U solutions and discuss the computational costs, the number of breakpoints, the effect of time horizon on the solution quality and the sensitivity analysis with larger scale problems in Case 2. Fourth, three real-world examples with historical data from the NCA are presented in Case 3.

5.1 Computational Settings

We limit the set $\bar{\Omega}$ to those scenarios with exactly one distress call and also only consider one possible drift trajectory for each vessel in distress. The first assumption is reasonable as distress calls are quite rare. The second assumption is a simplification that places focus on the main source of uncertainty: time of distress call (Ni et al., 2010). A richer set of scenarios are easily included but its generation is beyond the scope of the paper. In Cases 1 and 2, the drift trajectories are randomly generated using a Markov chain. Specifically, we subdivide the region into 20 zones, where the sum of the wind and current force direction ($U_w + U_C$) for each zone is either north-east, north-west or north-south. Each zone is randomly associated with one of these three directions. Additionally, every cell in the region is directly connected from below with three cells, which are named Left, Straight and Right. The next cell in the path $p = (c_t, \dots, c_T)$ of a drifting vessel scenario is randomly determined based on the zone where the current cell falls (see Table 1). For instance, if the current cell is located in the zone where the vector $U_w + U_C$ has a north-east direction, then the Left cell will be chosen as next cell in the path with a probability equal to 0.25. In addition, the wave magnitude at each cell is randomly given a value of 0 or 1 with equal probabilities, where the value of 0 represents low wave height and 1 that of large wave magnitude. The drifting vessel will spend two time periods at cells with large wave magnitude and only one time period at cells with small wave height. In Case 3, historical wave height, current and wind forces are used to determine each drift trajectory; see further details in Subsection 5.4.

Previous study in the Norwegian sea propose an average failure rate of 0.26 per ship-year (Hansson and Kiær, 1997). The research is not based on actual statistics but on a fault tree analysis, combining failure rates for components and expert judgment. It is not clear how these results can be implemented for different ships in a simulation experiment. Additionally, these data are old and may not be representative for today's accident scenarios. In the paper, these probabilities of failure are randomly generated with very low values at every time periods to reflect the actual scenarios. In the case studies with historical events, we have computed these probabilities based on the frequency of drift accidents but still include some randomness. Specifically, let p_s be the drifting rate for a specific period of time in the region of interest.

Then we generate the probabilities of failure, R_{ω_v} , for every vessel such that $p \in [0.01, 0.09]$ and $R_{\omega_v} = \frac{P}{p_s}, \sum R_{\omega_v} = p_s$, where $1 - p_s$ is the probability of no failure. Further challenging analytical and empirical researches are needed to effectively determine these probabilities. Nevertheless, we have done some sensitivity analysis with different distributions, which include different values of R_{ω_v} . Furthermore, the grounding cost for each vessel scenario is computed using the formula $K = 51.432V^{0.728}$, where the volume V is randomly generated according to a uniform random variable on $[2187, 51704]$ plus a normal random variable with mean 15000 and standard deviation = 5000 (see Kontovas et al. (2010) for details on grounding costs and volume of oil spills). Moreover, the VTS center in Vardø currently operates with two tugboats. We use this number of tugboats for experiments in all the three cases. These tugboats have a secondary function of escorting vessels that are in transit to Norwegian ports. Thus, they are required to move relatively close to shore as reflected in our discretization of the area of interest and movement constraints. The problem of whether the resource capacity are optimal or not is out of the scope of this paper. We propose an optimal tugs policy based on the resource available. However, the fleet of tug was reduced from three to two a year ago by the NCA and could be justified by few main reasons. First, the accidents are very rare and most of the drift time are very long with 20 to 30 hours (slow drift) and fast drift count for only 10 hours Eide et al. (2007). Second, The NCA have acquired "ship arrestors", which considerably reduce the vessel's drifting speed and give more time to the tugs to hook-up with the vessel in time.

All computations are carried out on a personal computer with an Intel(R) Pentium(R) IV 3.0 CPU and 4.0 GB of RAM, running Windows 7. The optimization solver is Gurobi 5.5.0.

Table 1: Transition probabilities for path generation

$U_w + U_C$	North-east			North-west			North-south		
Cell	Left	Straight	Right	Left	Straight	Right	Left	Straight	Right
Prob	0.25	0.25	0.5	0.5	0.25	0.25	0.25	0.5	0.25

5.2 Case 1: Illustrative Example

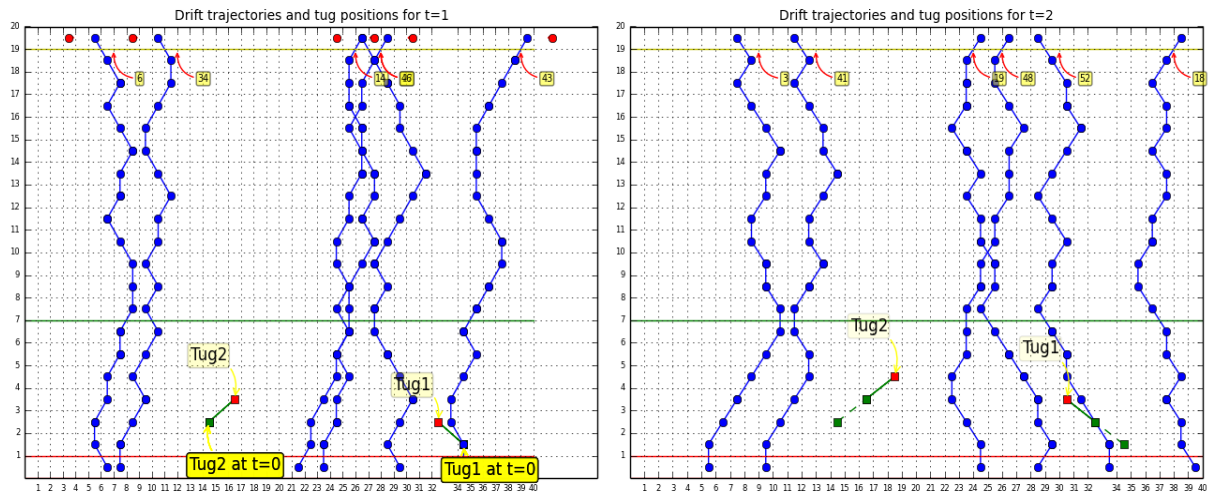
We start by considering a corridor of length 40 kilometers and width 20 kilometers divided into 800 cells of 1-by-1 kilometer. Six vessels sail in the corridor 18 km off the coastline. These vessels are patrolled by two tugboats moving close to shore with a maximal speed of 10.7 knots (1 knot= 1.85 km/h). Each vessel moves in the corridor with an average speed between 6.5 and 19.5 knots. Moreover, a planning horizon of 6 hours is used with a time step of one hour. For this case, tugboats are constrained to move relatively slowly. Each cell c has a total of 15 reachable cells in $\mathcal{F}_{t_g}(c)$, which represents the number of possible hops per time period. Figure 3 shows an optimal solution, where tugboats are represented by small squares and are allowed to move between shore and the green line. Tug2 is initially positioned 3 km

off the coast and 15 km from the origin point with coordinate (0,0) in the figure, while Tug1 is positioned 2 km away from the coast and 34 km from the origin point along the coast. The optimal positions of tugboats are also shown in Figure 3. In addition, the initial position of each vessel is represented by a red circle and the vessel scenarios for each time period as blue circles linked with blue sticks. Moreover, the corridor is delimited by a yellow line and the coast is shown by a red line. The cost, in million NOK, for each vessel scenario is labeled close to each drift trajectory. The number of scenarios, $|\bar{\Omega}|$, is equal to 36 for six vessels and six time periods. For every time period, Figure 3 illustrates the optimal decision of the model and the potential drift trajectories. In the figure for time period t , we only show the six drift trajectories that are associated with a distress call at t .

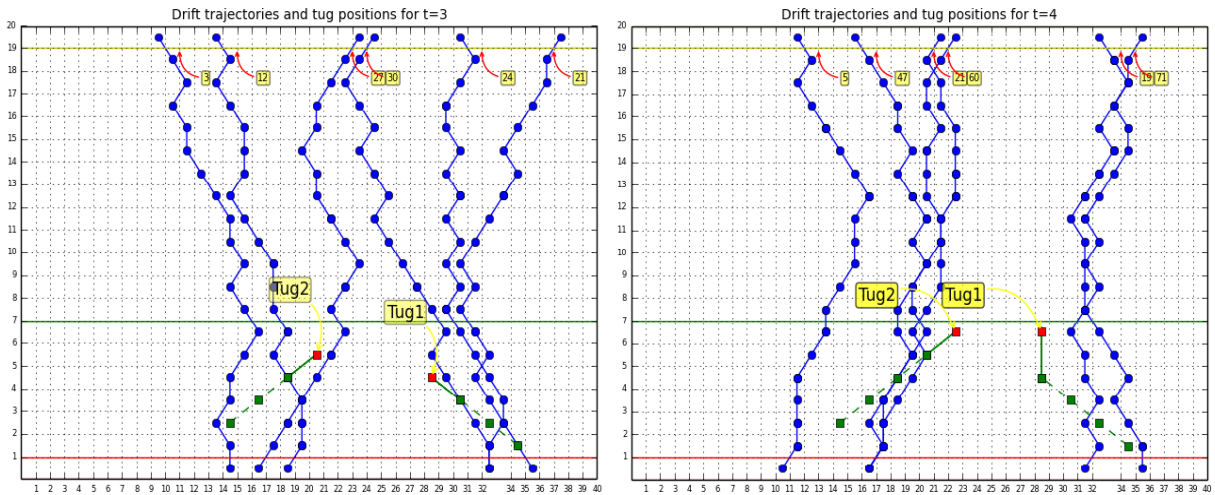
Both MIP-L and MIP-U give the same objective value of NOK 0.67 million as well as tugboat positions at each time period. This optimal solution is obtained in 15 seconds for MIP-U and 170 seconds for MIP-L. For this test instance, MIP-L model has a total number of 60,765 constraints and 36 continuous variables, whereas MIP-U has a total number of 825 constraints and 36,000 continuous variables. The two models have the same number of binary variables of 2,880. At each time period in the planning horizon, the optimal decisions are influenced by the vessel scenarios of the next time periods. This is well illustrated in period 2, where Tug2 moves slightly away from the path with high cost of NOK 41 million. In fact, there are more scenarios with considerable cost on the east side of Tug2 both in periods 2, 3 and 4. Additionally, if we consider only vessel scenarios at the fourth time period, it might not be optimal to move Tug2 east, which is actually optimal when considering vessel scenarios in the next time periods. As expected, the tugboats move towards the corridor until they reach the green line limit (see Figure 3). The closer the tugboats move away from the coastline, the greater the probability of successful hook-up of potential drifting vessels.

5.3 Case 2: Computational Tests

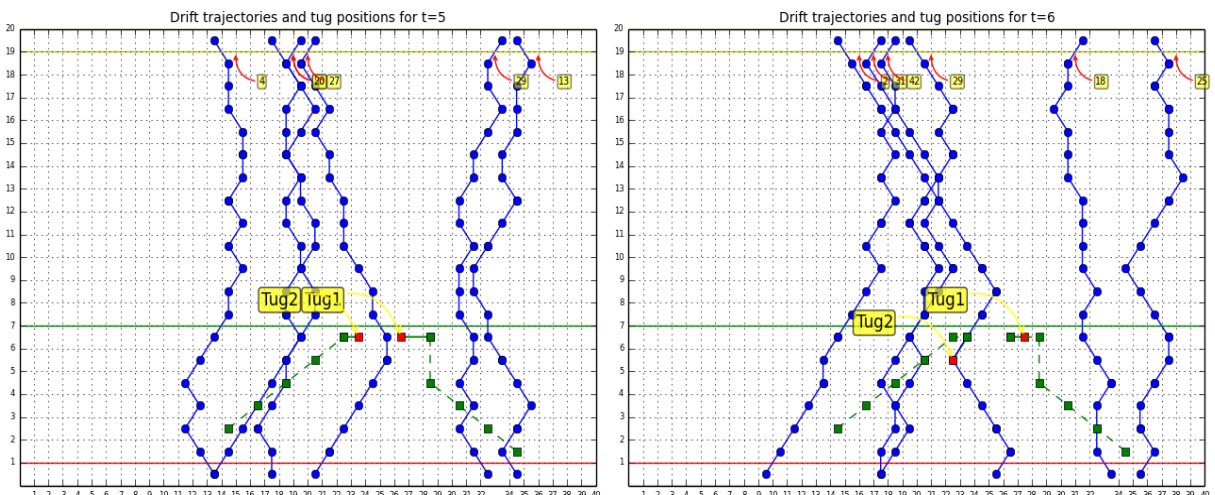
To evaluate the performance and quality of the models developed, we present results for realistically sized test instances. The cells for this case are built with geographical positions from the region of interest for the VTS. Clearly, we collect the geographical coordinates of the center position of each cell and transform them into Cartesian coordinates for calculations. Once the model is run, the optimal positions of tugboats as well as drift trajectories and vessels positions are transformed back to geographical coordinates. The region of interest covers about 1,100 km of coastline and the corridor is on average 50 km off the coastline. We partition the area between the corridor and the coastline into cells of 5 by 5 km, which gives a total number of 2,200 cells. In practice, the number of cells is slightly smaller than the number given above. This is explained by the fact that the corridor and the coastline are not straight lines and neither totally parallel to each other. Thus, we use few triangle cells with different sizes to better represent the region of interest. Vessels typically have an operating speed of 14 to 15 knots and



(a) Results for periods 1 and 2



(b) Results for periods 3 and 4



(c) Results for periods 5 and 6

Figure 3: Results for Case1: Illustrative Example. The green and blue solid lines represent the movement of tugboats and drift trajectories of vessels, respectively.

tugboats about 12 knots (Eide et al., 2007). In addition, the operators have subdivided the region of interest into two zones. The first tugboat is assigned to the first zone, Zone A, spanning from the border to Russia to Torsvåg, and Zone B from Torsvåg to Røst is patrolled by the second tugboat.

5.3.1 Case 2A: Many Breakpoints

In this subsection, we mainly compare the MIP-U and MIP-L models with regards to solution quality and run time, and present the gap between the optimal OTP value and optimal MIP-U or MIP-L values. Accordingly, a test set of 6 vessels and 2 tugboats over a period of 20 hours with one hour time steps are randomly generated. In this test set, the tugboats cannot move more than 25 km away from the shore. That is, the patrol zone accounts for about 1,100 cells along the coastline. The test case constitutes 30 instances and the results for the two MIPs are presented in Table 2. The run time is in minutes and the objective function in million NOK.

Preliminary calculations indicate that $K = 1,000$ is the minimum number of breakpoints in MIP-L and MIP-U, that gives an optimal solution of OTP. Consequently, we use 2,000 breakpoints in order to be highly confident that MIP-L and MIP-U give the optimal solutions of the OTP model. For each instance, the total number of binary variables for both MIPs are 22,974 with 120 and 240,000 continuous variables respectively for MIP-L and MIP-U. The total number of constraints for MIP-L is 261,924 and 22,045 for MIP-U.

As presented in Table 2, the MIP-U model is about 93 times faster than MIP-L. Additionally, the variability in run times for MIP-L is larger than that of MIP-U. The average solution value is NOK 0.5797 million for MIP-U and NOK 0.5792 for MIP-L. Although the objective values of the two MIPs are slightly different, the optimal decisions for the tugboat positions are the same for every test result. In addition, the relative optimality gap defined by $(\min\{f(\bar{\mathbf{x}}), f(\underline{\mathbf{x}})\} - \text{MIP-L})/\text{MIP-L}$ is the negligible 0.03%, with a maximum of 0.05%.

Table 2: Case 2A. Test results for 30 instances

$$\text{GAP} = (\min\{f(\bar{\mathbf{x}}), f(\underline{\mathbf{x}})\} - \text{MIP-L})/\text{MIP-L}$$

	MIP-U		MIP-L		$\min\{f(\bar{\mathbf{x}}), f(\underline{\mathbf{x}})\}$	%GAP
	Obj.Val	Time (min)	Obj.Val	Time (min)		
Avrg	0.5797	7.57	0.5792	707.07	0.5796	0.029
Std.dev	0.3955	10.43	0.3954	95.42	0.3955	0.019
Min	0.1251	1.49	0.1250	573.72	0.1251	0.006
Max	1.5497	52.18	1.5485	888.63	1.5493	0.052

5.3.2 Case 2B: Few Breakpoints

The choice of 2000 breakpoints leads to optimal tugboat positions in all instances examined at the expense of high run times. As presented in Table 2, it takes between 1.5 and 52.2 minutes

to obtain a solution of MIP-U, and even longer for MIP-L. In order to assess the solution quality with relatively few breakpoints, the two MIPs models are run with another set of 50 instances in the same manner as in Case 2A, with 500 breakpoints for MIP-U and 200 for MIP-L. This gives a total number of 82,974 variables and 22,045 constraints for MIP-U, and 23,094 variables with 45,924 constraints for MIP-L.

The average relative optimality gap is 0.51%, with a maximum of 5.4% (see Table3). The solution are obtained in 1.99 minute and 13.17 minutes on average for MIP-U and MIP-L, respectively. Moreover, the runtime for MIP-U is less than 9 minutes for every test instance. The MIPs are able to obtain optimal decisions on tugboat positions for 15 instances out of 50. Although the number of vessels are the same for each instances, the initial vessel positions along the corridor are different for each test case. Consequently, the number of scenarios varies for every test instance. Clearly, some vessels might leave the region before the end of the planning horizon, and thus reduce the number of vessel scenarios. This explains the high standard deviation both on the objective values and runtime presented in Table 3. However, these results remain practically reasonable as one might run the model every hour within a receding horizon framework discussed in the next subsection.

Table 3: Case 2B. Test results for 50 instances with small number of breakpoints $GAP = (\min\{f(\bar{\mathbf{x}}), f(\underline{\mathbf{x}})\} - \text{MIP-L}) / \text{MIP-L}$

	MIP-U		MIP-L		$\min\{f(\bar{\mathbf{x}}), f(\underline{\mathbf{x}})\}$	%GAP
	Obj.Val	Time (min)	Obj.Val	Time (min)		
Avrg	0.6901	1.9958	0.6855	13.1669	0.6886	0.5152
Std.dev	0.7139	1.9709	0.7092	7.0475	0.7120	0.9421
Min	0.1762	0.1517	0.1746	2.4903	0.1757	0.0003
Max	2.0669	8.4818	2.0560	26.9707	2.0616	5.4455

5.3.3 Case 2C: Effect of Time Horizon

The number of scenarios increases with the length of the planning horizon. We use one large test instance from Case 2A and run the MIP models for different planning horizons, ranging from two to 22 hours. The result in Figure 4 shows how the computational time increases with the length of the time horizon and highlights the run times performance of MIP-U compared to that of MIP-L. Furthermore, it is clear from Figure 4 that MIP-U better copes with larger instance size than MIP-L. However, MIP-L is of course essential in computing a relative optimality gap.

The weather forecast is available in real time at the VTS center and dynamic information from vessels are transmitted on average every 2 seconds (Eide et al., 2007). This information can be used for repeated updates of the model resulting in better predictions of future vessel scenarios; see for example Park et al. (2009) and Wang et al. (2007) for background on such receding horizon control. Accordingly, MIP-U could be run in real time, with parameters updated

every time period. For instance, the model could be run for 20 hours, while only the first hour is being implemented. Then we update the parameters and run the model again for the next 20 hours and so forth.

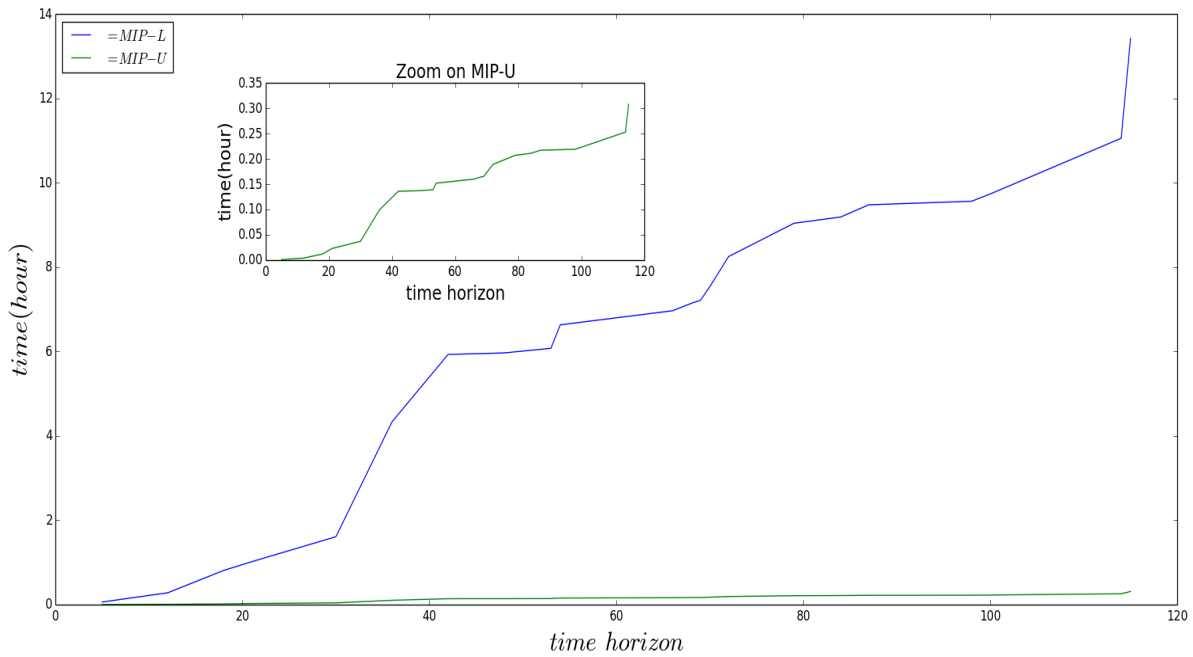


Figure 4: Case 2C. Influence of the number of scenarios on the computational time. The blue solid line represents the performance of the MIP-L model and the green solid line is that of the MIP-U model.

5.3.4 Case 2D: Sensitivity Analysis with Larger Scale Problems

To analyze the sensitivity of the MIP-U model as well as its scalability, we run different test instances with a total of 10 vessels for a number of tugboats ranging from one to six. For each number of tugboats and distribution of drift trajectories, we run the MIP-U model and compare its solution value with two different distributions for the same tugboat positions. These settings allow us to analyze the sensitivity of the solution value to different probabilities of failure R_{ω_v} , grounding costs K_{ω_v} for each vessel scenario and fleet size.

In Figure 5, the green solid line represents the optimal cost distribution while the red and blue solid lines represent the variation of the expected cost for two different distribution of drift trajectories. Unsurprisingly, the solution values are very sensitive with changes in the failure probabilities and grounding costs. This is mainly due to the high uncertainty about weather conditions and ocean currents. Although the integration of the MIP-U model with the receding horizon control algorithm, described in Section 4.2, could considerably address this issue, more accurate parameters estimation are required. Additionally, the expected environmental cost obviously decreases with higher number of tugboats as shown in Figure 5. Increasing the fleet size will bring additional acquisition costs, which are strategic decisions not discussed in this paper. Our model, however, focuses on operational decision level by proposing optimal real-

time allocation and positioning of tugboats based on the available fleet size. Nevertheless, the NCA has decided to reduce the speeds of drifting vessels by acquiring new "ship arrestors" and reduce its fleet size from three to two tugboats. Moreover, the maximum runtime for these larger scale instances is less than 45 minutes, which is sufficient to run the model every one or two hours with the receding horizon control algorithm. Sophisticated heuristics algorithms might reduce this computing time further. For cases where larger fleet sizes are needed, this scalability issue can also be easily addressed by subdividing the region of interest into smaller zones and optimally assign tugboats to each zone. The new problem will then be very similar to that of the location/allocation and deployment of ambulances in the EMS systems.

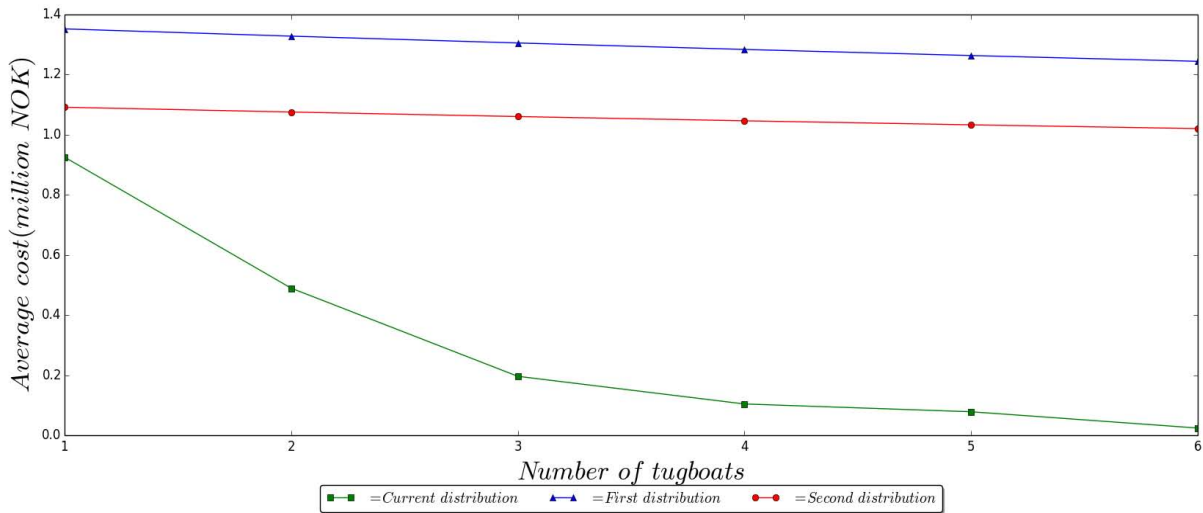


Figure 5: Case 2D. Influence of the number of tugboats and distributions of the drift trajectories on the expected environmental cost. The green solid line represents the optimal costs for the current distribution while the red and blue solid lines represent the variation in the costs with different distributions.

5.4 Case 3: Historical Events

In this subsection, we discuss three real-world cases with historical data from the NCA. Case 3A involves no grounding incident, but highlights the potential cost saving opportunities that could be gained by having solutions of the OTP problem guide decisions. In Cases 3B and 3C, we present two different instances where an accident actually occurred and run the model for 15 hours prior to the time of distress.

A path $p = (c_1, \dots, c_T)$ for each vessel scenario ω_v is generated using AIS and NMI information with the algorithm presented in Section 4.2. Specifically, we collect the wind and current velocities, and wave force of the center point of each cell at each time period of the planning horizon and use the algorithm described in Section 4.2. to generate a path for each vessel scenario ω_v . In addition, the number of vessels in the region and their geographical positions for every time period, the time of distress and grounding locations are collected from AIS. Moreover, we use the basemap library in python to plot and draw the map with vessel scenarios and

tugboat positions.

5.4.1 Case 3A: May 7, 2014

On the 7th of May 2014, six vessels sailed along the coastline of the High North. Their initial positions, speed over the ground (SOG) and direction at 1:30am are given in Table 4. At each time period of one hour, a potential vessel scenario is randomly generated, based on the historical wind and current directions and the model presented in Section 4.2, for every vessel. The problem size for this case is the same as Case 2A.

Table 4: Case 3A. Initial vessel positions and speeds

	Vessel 1	Vessel 2	Vessel 3	Vessel 4	Vessel 5	Vessel 6
Direction	North-west	West-north	West-north	North-west	West-north	North-west
Latitude	$N68^{\circ}02$	$N68^{\circ}15$	$N68^{\circ}21$	$N71^{\circ}07$	$N71^{\circ}22$	$N70^{\circ}38$
Longitude	$E009^{\circ}44$	$E010^{\circ}34$	$E010^{\circ}50$	$E019^{\circ}24$	$E021^{\circ}49$	$E032^{\circ}10$
SOG	12.4	10.5	13.7	13.2	11.5	13.3

The optimal solution for MIP-U was found in 5.6 minutes with an objective value of NOK 0.34 million. The actual events had the first tug boat located at $70^{\circ}58'N - 025^{\circ}51'E$ and the second one at $69^{\circ}40'N - 018^{\circ}59'E$, and they were stationary during the whole planning horizon of 20 hours in accordance with current VTS policy.

The optimal locations for the first six time periods are presented in Figure 6. The priority is given to vessel scenarios with high cost. In the first time period, Tug2 moves north because of the high costs located in that direction. Tug1 moves west toward a vessel with small cost of NOK 15 millions in period 4, leaving a vessel with higher cost of NOK 41 millions, but this is due to the high cost of NOK 82 and NOK 51 million that appear in periods 5 and 6, respectively.

In this instance where no accident happened, the real cost was of course equal to zero. However, the expected cost under this policy is actually NOK 0.75 million, significantly higher than the optimized of NOK 0.34 million.

5.4.2 Case 3B: March 21, 2014

On the 21st of Mars 2014 at 11:10pm, a vessel ran aground at $71^{\circ}01.06'N - 028^{\circ}27.46'E$ after about 15 hours of drifting time. At the time of distress, 07:55am, the nearest tugboat was located at $70^{\circ}40'N - 023^{\circ}40'E$, and was not able to reach the drifting vessel on time. The tugboat moved toward the vessel but was 142.8 km away at the time of grounding. We run the MIP-U model with this case for 15 hours prior to the time of distress and present the results for the first and last time periods in Figure 7. The blue lines in Figure 7 represent the predicted drift trajectories for all the vessels that moved into the region in that time horizon, including the one that ran ashore, while the actual path followed by the drifting vessel is presented in green solid line. The two directed paths in red solid lines are the actual positions of tugboats from

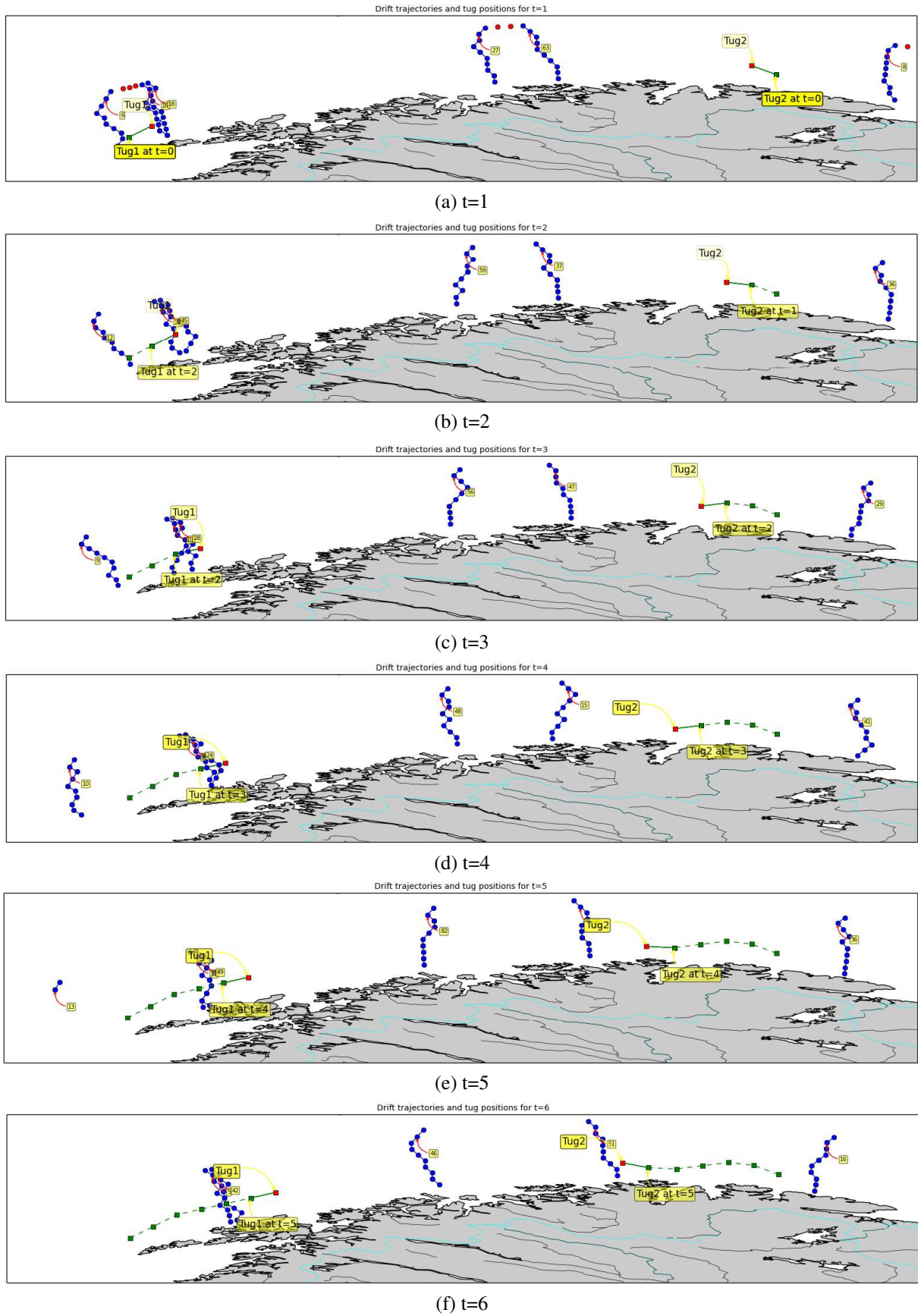


Figure 6: Case 3A. Illustration of the first six time periods. The dashed green lines represent tugboat movements at each time period and the blue solid lines represent vessel trajectories.

the time of distress to the time of grounding and the paths in dashed green line are suggested positions of tugboats by the model prior to the distress call. It is important to note that, in these green paths, the last positions represent the location of tugboats at time of distress of the vessel that ran ashore, not at the grounding time. A zoomed-in view of the grounding location of the drifting vessel as well as the nearest tugboat (Tug1) are presented in Figure 8, where the distance between the predicted and actual grounding location is about 17 km. Although this value is not large, further research as highlighted in the last section, needs to be done for accurate drift trajectories.

The probability of successful hook-up of the grounded vessel by Tug1 with the predicted drift trajectory and the MIP-U model is 0.79 and that of the actual drift trajectory is equal to 0.86. That is, the grounded vessel had 86% chance to be rescued if the MIP-U model was implemented at that time. Based on the actual position of Tug1 at time of distress from the current policy (see the first position of the red path in Figure 8) the vessel had only 0.22 probability to be hooked-up. For this real-world instance, the expected cost is equal to NOK 0.19 million if using the OTP model and NOK 0.28 million for the actual movement of tugboats.

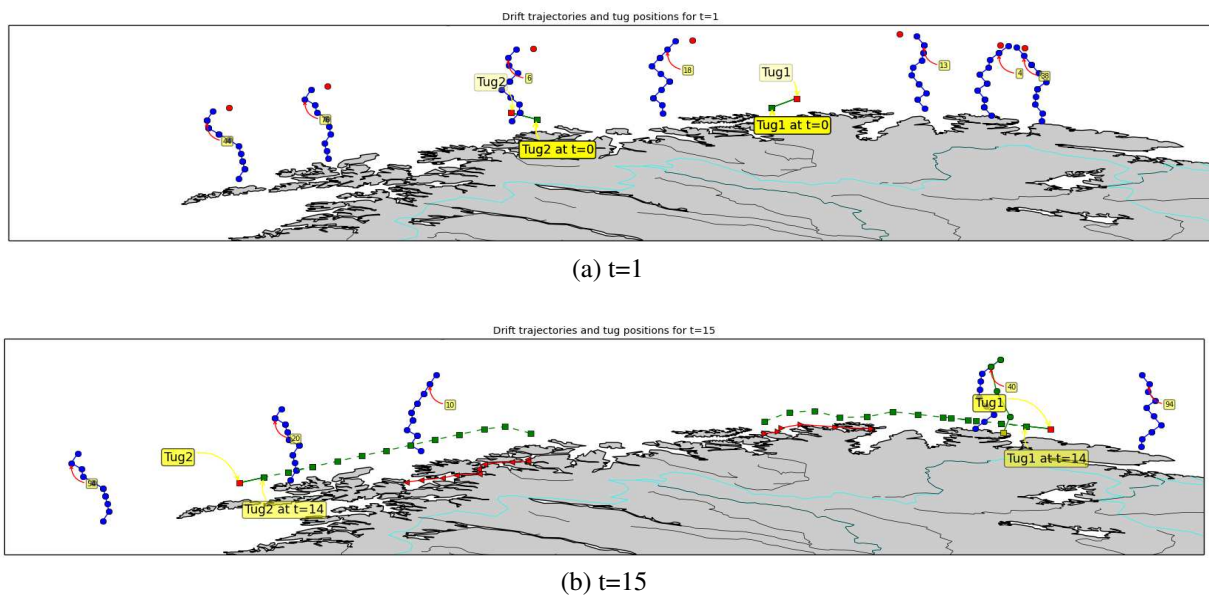


Figure 7: Case 3B. Results for the first instance with grounded vessel. The dashed green lines represent the suggested movements of tugboats by the MIP-U model and the predicted drift trajectories in blue solid lines. In addition, the actual drift trajectory of the vessel that ran aground is represented by green solid lines. The paths in red are the actual positions of tugboats from the time of distress to the time of grounding.

5.4.3 Case 3C: September 12, 2014

In this case, a vessel ran ashore at $71^{\circ}02.97'N - 023^{\circ}53.89'E$ on September 12 2014 at 2:25pm. The nearest tugboat, located at $70^{\circ}41.58'N - 023^{\circ}19.21'E$, stayed static for the whole drifting time of about 9 hours. As explained by the operators at the VTS center, vessels are

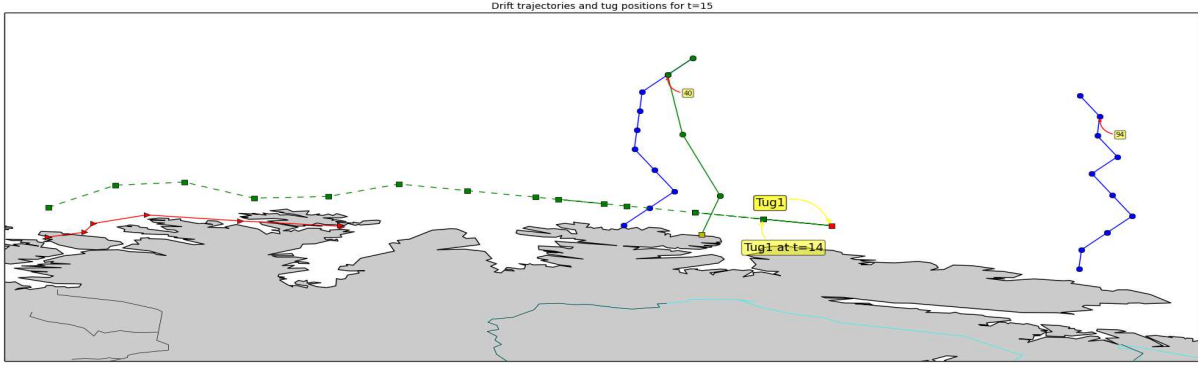
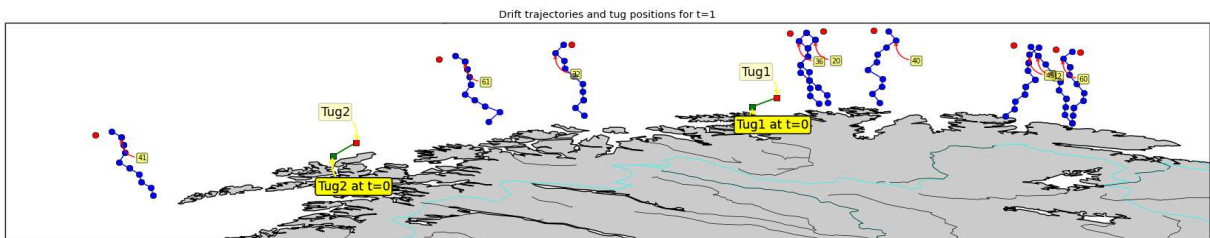
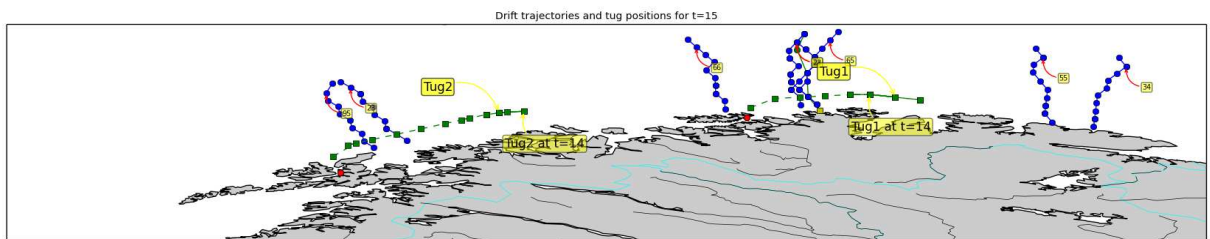


Figure 8: Zoom on the grounded vessel for case 3B. The dashed green lines represent the suggested movements of the nearest tugboat by the MIP-U model and the predicted drift trajectories are represented in blue solid lines. In addition, the actual drift trajectory of the vessel that ran aground is represented in green solid lines. The path in red is the actual positions of the nearest tugboat from the time of distress to the time of grounding and the estimated grounding cost in million NOK for each drift trajectory is labeled in yellow.

not given the same priority and sometimes vessels moving out of the corridor will “misinform” the VTS center that they are not in trouble but merely fishing (or some other false message) while they are in fact drifting with the risk of grounding. This peculiar situation often stems from misunderstandings about the cost of rescue to the ship owner. The rescue is in fact free for the ship owner, but this is not widely known. The MIP-U model is also run for 15 hours prior to the time of distress of the grounding vessel. The results for the first and last time periods



(a) t=1



(b) t=15

Figure 9: Results for Case 3C. The dashed green lines represent the suggested movements of the tugboats by the MIP-U model and the predicted drift trajectories are represented in blue solid lines. In addition, the actual drift trajectory of the vessel that ran aground is represented in green solid lines. The two cycles in red are the actual static position of the tugboats from the time of distress to the time of grounding and the estimated grounding cost in million NOK for each drift trajectory is labeled in yellow.

are presented in Figure 9 and the zoom on the grounding location is presented in Figure 10,

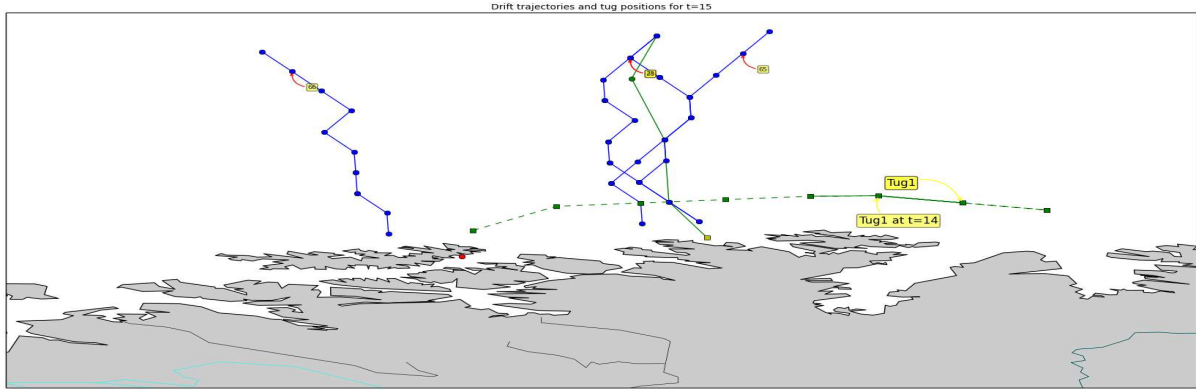


Figure 10: Zoom on the grounded vessel for case 3C. The dashed green lines represent the suggested movements of the nearest tugboat by the MIP-U model and the predicted drift trajectories are represented in blue solid lines. In addition, the actual drift trajectory of the vessel that ran aground is represented in green solid lines. The cycle in red is the actual static position of the nearest tugboat from the time of distress to the time of grounding and the estimated grounding cost in million NOK for each drift trajectory is labeled in yellow.

where the red circle represents the position of the nearest tugboat. The predicted drift trajectory has a grounding position 43 km away from the location where the vessel actually ran aground. For this particular case, the model and the current policy have a close probability of successful hook-up of 0.79 and 0.69, respectively. This is mainly due to the actual static position of the tugboat and the grounding location, which in this case is rather fortunate. In addition, the MIP-U model does not know which drift will occur in advance and thus, tries to minimize the overall expected cost. Indeed, there are two drift trajectories with high costs on the right side of the nearest tugboat. This is why the tugboat does not move closer to the drift trajectory that actually occurred. The expected cost for this real-world instance is equal to NOK 0.07 million if using the OTP model and NOK 0.24 million for the current policy.

6 Conclusions

In this article, we developed a nonlinear binary integer programming model to minimize the clean-up costs, socioeconomic losses and environmental costs associated with oil spill from grounding accidents. Two linearizations of the model lead to mixed integer models that bound the optimal value of the original problem with practically near zero optimality gaps. The paper also presents methods for obtaining input data to the model. Preliminary results for small and realistically-sized instances indicate noteworthy features of our approach. Optimal tugboat positions are obtained in less than two minutes for realistic instances with a small number of breakpoints. A test with a real-world instance in Case 3A indicates a total clean-up and socioeconomic costs saving opportunity of 45%. Moreover, tests with three representative historical data sets highlight the importance and benefits of implementing the MIP-U model at the NCA. Specifically, we demonstrate that on a single day in 2014, decision support by the proposed

model might have reduced the expected cost from grounding accidents that day from NOK 0.75 million to NOK 0.34 million. In two other studies of actual grounding incidents in 2014, we predict that adoption of the decision support tool in the hours prior of the grounding events might have increased the probability of avoiding those accidents from 22% to 86% in the first incident and from 69% to 79% in the second. The NCA finds these estimates exceptionally interesting and the proposed decision support tool highly promising as the basis for a real-time automated system that can assist the NCA's VTS operators. Although the model is not yet implemented in practice, the examples use real data, which provide an indicate of what we can expect.

It is recommended that further studies are initiated in order to obtain more accurate input for the model. First, the region should be partitioned into an "optimal" number of cells. A large cell size will reduce the precision on tugboat positions as well as vessel scenarios. Conversely, small cells size gives good precision at the expense of high model complexity. Second, more than one vessel scenario at each time period and scenario could be considered, which might lead to a need for Monte Carlo sampling techniques. Third, and most importantly, there is a need for better assessments of grounding costs at each coastline segment as well as estimates of probabilities of distress calls. Furthermore, the model can be extended and incorporate a receding horizon control algorithm to effectively address the uncertainty and dynamic environment of the problem. In fact, there might be new vessels entering and leaving the region during the planning horizon. In addition, one of the tugboats could be out of patrol because of several reasons such as escort of vessels and crew shift. All this information needs to be updated dynamically. Finally, different objective functions could be used for the OTP problem. For instance, minimizing the superquantile instead of the expected cost could be of great interest to the NCA.

Acknowledgments

This work is carried out with partial funding from Aalesund University College and the Research Council of Norway through the project Dynamic Resource Allocation with Maritime Application (DRAMA), grant ES504913. We sincerely acknowledge Trond Ski at the Norwegian Coastal Administration (NCA) for his support and input during the work with this paper.

References

Abi-Zeid, Irène, John R. Frost. 2005. Sarplan: A decision support system for canadian search and rescue operations. *European Journal of Operational Research* **162**(3) 630 – 653. doi:<http://dx.doi.org/10.1016/j.ejor.2003.10.029>. URL <http://www.sciencedirect>.

- com/science/article/pii/S0377221703008166. Decision-Aid to Improve Organisational Performance.
- Afshartous, David, Yongtao Guan, Anuj Mehrotra. 2009. {US} coast guard air station location with respect to distress calls: A spatial statistics and optimization based methodology. *European Journal of Operational Research* **196**(3) 1086 – 1096. doi:<http://dx.doi.org/10.1016/j.ejor.2008.04.010>. URL <http://www.sciencedirect.com/science/article/pii/S0377221708003731>.
- Allen, Arthur A., Jeffrey V Plourde. 1999. Review of leeway: Field experiments and implementation. Tech. rep., US Coast Guard Research and Development Center Groton CT.
- Alpern, Steve, Shmuel Gal. 2002. Searching for an agent who may or may not want to be found. *Operations Research* **50**(2) 311–323.
- Andersson, T., P. Värbrand. 2007. Decision support tools for ambulance dispatch and relocation. *The Journal of the Operational Research Society* **58**(2) 195–201. URL <http://dx.doi.org/10.1057/palgrave.jors.2602174>.
- Assimizele, Brice, Johan Oppen, Robin T. Bye. 2013. A sustainable model for optimal dynamic allocation of patrol tugs to oil tankers. *Proceedings of the 27th European Conference on Modeling and Simulation*. 801–807.
- Badri, Masood A., Amr K. Mortagy, Colonel Ali Alsayed. 1998. A multi-objective model for locating fire stations. *European Journal of Operational Research* **110**(2) 243 – 260. doi:[http://dx.doi.org/10.1016/S0377-2217\(97\)00247-6](http://dx.doi.org/10.1016/S0377-2217(97)00247-6). URL <http://www.sciencedirect.com/science/article/pii/S0377221797002476>. {EURO} Best Applied Paper Competition.
- Balcik, B., B. M. Beamon. 2008. Facility location in humanitarian relief. *International Journal of Logistics Research and Applications* **11**(2) 101–121. doi:10.1080/13675560701561789. URL <http://www.tandfonline.com/doi/abs/10.1080/13675560701561789>.
- Basdemir, M. Melih. 2004. Locating search and rescue stations in the aegean and western mediterranean regions of turkey. *Journal of aeronautics and space technologies* **1**(3) 63–76.
- Bazaraa, M. S., H. D. Sherali, C. M. Shetty. 1995. *Nonlinear Programming—Theory and Algorithms*. 2nd ed. John Wiley & Sons.
- Beasley, J.E., K. Jørnsten. 1992. Practical combinatorial optimization enhancing an algorithm for set covering problems. *European Journal of Operational Research* **58**(2) 293 – 300. doi:[http://dx.doi.org/10.1016/0377-2217\(92\)90215-U](http://dx.doi.org/10.1016/0377-2217(92)90215-U). URL <http://www.sciencedirect.com/science/article/pii/037722179290215U>.

- Breivik, Oyvind, Arthur A. Allen. 2008. An operational search and rescue model for the norwegian sea and the north sea. *Journal of Marine Systems* **69**(1–2) 99 – 113.
- Bye, Robin T. 2012. A receding horizon genetic algorithm for dynamic resource allocation: A case study on optimal positioning of tugs. *Series: Studies in Computational Intelligence* **399** 131–147. Springer-Verlag: Berlin Heidelberg.
- Bye, Robin T., Hans G. Schaathun. 2014. An improved receding horizon genetic algorithm for the tug fleet optimisation problem. *Proceedings of the 28th European Conference on Modeling and Simulation*. 682–690.
- Bye, Robin T., Hans G. Schaathun. 2015a. Evaluation heuristics for tug fleet optimisation algorithms: A computational simulation study of a receding horizon genetic algorithm. *Proceedings of the 27th European Conference on Modeling and Simulation*. 270–282.
- Bye, Robin T., Hans Georg Schaathun. 2015b. A simulation study of evaluation heuristics for tug fleet optimisation problems. *Accepted for publication in Operations Research and Enterprise Systems. In Communications in Computer and Information Science*. Springer-Verlag: Berlin Heidelberg.
- Camacho-Collados, M., F. Liberatore. 2015. A decision support system for predictive police patrolling. *Decision Support Systems* **75** 25 – 37. doi:<http://dx.doi.org/10.1016/j.dss.2015.04.012>. URL <http://www.sciencedirect.com/science/article/pii/S0167923615000834>.
- Camacho-Collados, M., F. Liberatore, J.M. Angulo. 2015. A multi-criteria police districting problem for the efficient and effective design of patrol sector. *European Journal of Operational Research* **246**(2) 674 – 684. doi:<http://dx.doi.org/10.1016/j.ejor.2015.05.023>. URL <http://www.sciencedirect.com/science/article/pii/S0377221715004130>.
- Campbell, James F. 1996. Hub location and the p-hub median problem. *Operations Research* **44**(6) 923–935. doi:10.1287/opre.44.6.923.
- Capar, İbrahim, Burcu B. Keskin, Paul A. Rubin. 2015. An improved formulation for the maximum coverage patrol routing problem. *Computers and Operations Research* **59** 1 – 10. doi:<http://dx.doi.org/10.1016/j.cor.2014.12.002>. URL <http://www.sciencedirect.com/science/article/pii/S0305054814003232>.
- Caprara, Alberto, Paolo Toth, Matteo Fischetti. 2000. Algorithms for the set covering problem. *Annals of Operations Research* **98**(1) 353–371. doi:10.1023/A:1019225027893.
- Chircop, P.A., T.J. Surendonk, M.H.L. van den Briel, T. Walsh. 2013. A column generation approach for the scheduling of patrol boats to provide complete patrol coverage. *Proceedings of the 20th International Congress on Modelling and Simulation*. 1–6.

- Church, Richard, Charles ReVelle. 1974. The maximal covering location problem. *Papers of the Regional Science Association* **32**(1) 101–118. doi:10.1007/BF01942293. URL <http://dx.doi.org/10.1007/BF01942293>.
- Church, Richard L., Charles S. ReVelle. 1976. Theoretical and computational links between the p-median, location set-covering, and the maximal covering location problem. *Geographical Analysis* **8**(4) 406–415. doi:10.1111/j.1538-4632.1976.tb00547.x. URL <http://dx.doi.org/10.1111/j.1538-4632.1976.tb00547.x>.
- Church, Richard L., Maria P. Scaparra, Richard S. Middleton. 2004. Identifying critical infrastructure: The median and covering facility interdiction problems. *Annals of the Association of American Geographers* **94**(3) 491–502. doi:10.1111/j.1467-8306.2004.00410.x. URL <http://dx.doi.org/10.1111/j.1467-8306.2004.00410.x>.
- Dalton, Tracey, Di Jin. 2010. Extent and frequency of vessel oil spills in US marine protected areas. *Marine Pollution Bulletin* **60**(11) 1939 – 1945.
- D’Amico, Steven J., Shoou-Jiun Wang, Rajan Batta, Christopher M. Rump. 2002. A simulated annealing approach to police district design. *Computers and Operations Research* **29**(6) 667 – 684. doi:[http://dx.doi.org/10.1016/S0305-0548\(01\)00056-9](http://dx.doi.org/10.1016/S0305-0548(01)00056-9). URL <http://www.sciencedirect.com/science/article/pii/S0305054801000569>. Location Analysis.
- Davari, Soheil, Mohammad Hossein Fazel Zarandi, Ahmad Hemmati. 2011. Maximal covering location problem (mclp) with fuzzy travel times. *Expert Systems with Applications* **38**(12) 14535 – 14541. doi:<http://dx.doi.org/10.1016/j.eswa.2011.05.031>. URL <http://www.sciencedirect.com/science/article/pii/S0957417411008153>.
- Davidović, Tatjana, Dušan Ramljak, Milica Šelmić, Dušan Teodorović. 2011. Bee colony optimization for the p-center problem. *Computers and Operations Research* **38**(10) 1367 – 1376. doi:<http://dx.doi.org/10.1016/j.cor.2010.12.002>. URL <http://www.sciencedirect.com/science/article/pii/S0305054810002923>.
- Dawson, M. C., J. E. Bell, J. D. Weir. 2007. A hybrid location method for missile security team positioning. *Journal of Business and Management* **13** 5–17.
- Dewil, R., P. Vansteenwegen, D. Cattrysse, D. Van Oudheusden. 2015. A minimum cost network flow model for the maximum covering and patrol routing problem. *European Journal of Operational Research* **247**(1) 27 – 36. doi:<http://dx.doi.org/10.1016/j.ejor.2015.05.067>. URL <http://www.sciencedirect.com/science/article/pii/S0377221715004798>.
- Drezner, Z. 1984. The planar two-center and two-median problems. *Transportation Science* **18**(4) 351–361. doi:10.1287/trsc.18.4.351.

- Eide, Magnus S., Oyvind Endresen, Oyvind Breivik, Odd Willy Brude, Ingrid H. Ellingsen, Kjell Roang, Jarle Hauge, Per Olaf Brett. 2007. Prevention of oil spill from shipping by modelling of dynamic risk. *Marine Pollution Bulletin* **54**(10) 1619 – 1633.
- Espejo, Inmaculada, Alfredo Marín, Antonio M. Rodríguez-Chía. 2015. Capacitated p-center problem with failure foresight. *European Journal of Operational Research* **247**(1) 229 – 244. doi:<http://dx.doi.org/10.1016/j.ejor.2015.05.072>. URL <http://www.sciencedirect.com/science/article/pii/S0377221715004841>.
- Gendreau, Michel, Gilbert Laporte, Frédéric Semet. 2001. A dynamic model and parallel tabu search heuristic for real-time ambulance relocation. *Parallel Computing* **27**(12) 1641 – 1653. doi:[http://dx.doi.org/10.1016/S0167-8191\(01\)00103-X](http://dx.doi.org/10.1016/S0167-8191(01)00103-X). URL <http://www.sciencedirect.com/science/article/pii/S016781910100103X>. Applications of parallel computing in transportation.
- Goerlandt, Floris, Jakub Montewka. 2014. A probabilistic model for accidental cargo oil outflow from product tankers in a ship–ship collision. *Marine Pollution Bulletin* **79**(1–2) 130 – 144.
- Grey, Catherine J. 1999. The cost of oil spills from tankers: an analysis of IOPC fund incidents. *Proceedings of the 1999 international oil spill conference*. 7–12.
- Hodgins, Donald O, Raymond Y Mak. 1995. *Leeway dynamic study phase I : development and verification of a mathematical drift model for four-person liferafts*. Seaconsult Marine Research, Vancouver, B.C.
- Iannoni, Ana Paula, Reinaldo Morabito, Cem Saydam. 2009. An optimization approach for ambulance location and the districting of the response segments on highways. *European Journal of Operational Research* **195**(2) 528 – 542. doi:<http://dx.doi.org/10.1016/j.ejor.2008.02.003>. URL <http://www.sciencedirect.com/science/article/pii/S0377221708001902>.
- Ishfaq, Rafay, Charles R. Sox. 2010. Intermodal logistics: The interplay of financial, operational and service issues. *Transportation Research Part E: Logistics and Transportation Review* **46**(6) 926 – 949. doi:<http://dx.doi.org/10.1016/j.tre.2010.02.003>. URL <http://www.sciencedirect.com/science/article/pii/S1366554510000244>.
- ITOPF. 2013. The international tanker owners pollution federation. Tech. rep., ITOPF.
- Jankowski, Daniel F. 1992. Fluid mechanics. *Journal of Fluid Mechanics* **244** 722–725.
- Jarvis, J. P. 1985. Approximating the equilibrium behavior of multi-server loss systems. *Management Science* **31**(2) 235–239. doi:10.1287/mnsc.31.2.235.

- Keskin, Burcu B., Shirley (Rong) Li, Dana Steil, Sarah Spiller. 2012. Analysis of an integrated maximum covering and patrol routing problem. *Transportation Research Part E: Logistics and Transportation Review* **48**(1) 215 – 232. doi:<http://dx.doi.org/10.1016/j.tre.2011.07.005>. URL <http://www.sciencedirect.com/science/article/pii/S1366554511000895>. Select Papers from the 19th International Symposium on Transportation and Traffic Theory.
- Kontovas, Christos A., Harilaos N. Psaraftis, Nikolaos P. Ventikos. 2010. An empirical analysis of IOPCF oil spill cost data. *Marine Pollution Bulletin* **60**(9) 1455 – 1466.
- Kum, Serdar, Bekir Sahin. 2015. A root cause analysis for arctic marine accidents from 1993 to 2011. *Safety Science* **74** 206 – 220. doi:<http://dx.doi.org/10.1016/j.ssci.2014.12.010>. URL <http://www.sciencedirect.com/science/article/pii/S0925753514003324>.
- Lecklin, Tiina, Riitta Ryömä, Sakari Kuikka. 2011. A bayesian network for analyzing biological acute and long-term impacts of an oil spill in the gulf of finland. *Marine Pollution Bulletin* **62**(12) 2822 – 2835.
- Lee, S. 2011. The role of preparedness in ambulance dispatching. *The Journal of the Operational Research Society* **62**(10) 1888–1897. URL <http://www.jstor.org/stable/23412422>.
- Li, S. (Rong), B. B. Keskin. 2013. Bi-criteria dynamic location-routing problem. *J Oper Res Soc* **65**(11) 1711–1725. URL <http://dx.doi.org/10.1057/jors.2013.116>.
- Lin, Ming-Hua, John Gunnar Carlsson, Dongdong Ge, Jianming Shi, Jung-Fa Tsai. 2013. A review of piecewise linearization methods. *Mathematical Problems in Engineering* 8doi:doi:10.1155/2013/101376.
- Lou, Yingyan, Yafeng Yin, Siriphong Lawphongpanich. 2011. Freeway service patrol deployment planning for incident management and congestion mitigation. *Transportation Research Part C: Emerging Technologies* **19**(2) 283 – 295. doi:<http://dx.doi.org/10.1016/j.trc.2010.05.014>. URL <http://www.sciencedirect.com/science/article/pii/S0968090X10000987>. Emerging theories in traffic and transportation and methods for transportation planning and operations.
- Majzoubi, Farshad, Lihui Bai, Sunderesh S. Heragu. 2012. An optimization approach for dispatching and relocating ems vehicles. *IIE Transactions on Healthcare Systems Engineering* **2**(3) 211–223. doi:10.1080/19488300.2012.710297. URL <http://dx.doi.org/10.1080/19488300.2012.710297>.
- Mišković, Stefan, Zorica Stanimirović, Igor Grujičić. 2015. An efficient variable neighborhood search for solving a robust dynamic facility location problem in emergency service

- network. *Electronic Notes in Discrete Mathematics* **47** 261 – 268. doi:<http://dx.doi.org/10.1016/j.endm.2014.11.034>. URL <http://www.sciencedirect.com/science/article/pii/S1571065314000766>. The 3rd International Conference on Variable Neighborhood Search (VNS'14).
- Millar, Harvey H., Suzana N. Russell. 2012. A model for fisheries patrol dispatch in the canadian atlantic offshore fishery. *Ocean and Coastal Management* **60** 48 – 55. doi:<http://dx.doi.org/10.1016/j.ocecoaman.2012.01.001>. URL <http://www.sciencedirect.com/science/article/pii/S0964569112000038>.
- Mokhtari, Kambiz, Jun Ren, Charles Roberts, Jin Wang. 2011. Application of a generic bow-tie based risk analysis framework on risk management of sea ports and offshore terminals. *Journal of Hazardous Materials* **192**(2) 465 – 475. doi:<http://dx.doi.org/10.1016/j.jhazmat.2011.05.035>. URL <http://www.sciencedirect.com/science/article/pii/S0304389411006741>.
- Ni, Zao, Zhiping Qiu, T.C. Su. 2010. On predicting boat drift for search and rescue. *Ocean Engineering* **37**(13) 1169 – 1179.
- Oghovese, Ogbereyivwe, Ogundele Suraju Olaniyi. 2014. On optimal allocation of crime preventing patrol team using dynamic programming. *International Journal of Mathematics and Statistics Invention* **2**(8) 07 – 17.
- Pal, Raktim, Indranil Bose. 2009. An optimization based approach for deployment of roadway incident response vehicles with reliability constraints. *European Journal of Operational Research* **198**(2) 452 – 463. doi:<http://dx.doi.org/10.1016/j.ejor.2008.09.010>. URL <http://www.sciencedirect.com/science/article/pii/S0377221708007534>.
- Park, Yeonjeong, Jeff S. Shamma, Thomas C. Harmon. 2009. A receding horizon control algorithm for adaptive management of soil moisture and chemical levels during irrigation. *Environmental Modelling and Software* **24**(9) 1112 – 1121.
- Pelot, Ronald, Amin Akbari, Li Li. 2015. *Applications of Location Analysis*, chap. Vessel Location Modeling for Maritime Search and Rescue. Springer International Publishing, Cham, 369–402. doi:10.1007/978-3-319-20282-2_16. URL http://dx.doi.org/10.1007/978-3-319-20282-2_16.
- Pietz, Jesse, J. O. Royset. 2014. Optimal search and interdiction planning. *In review*. .
- Psaraftis, Harilaos N., Geverghese G. Tharakan, Avishai Ceder. 1986. Optimal response to oil spills: The strategic decision case. *Operations Research* **34**(2) 203–217.
- Radovilsky, Z., T. Koermer. 2007. Allocation of us coast guard boats utilizing integer programming. *Journal of the Academy of Business and Economics* **7**(2) 130–135.

- Rajagopalan, Hari K., Cem Saydam, Jing Xiao. 2008. A multiperiod set covering location model for dynamic redeployment of ambulances. *Computers and Operations Research* **35**(3) 814 – 826. doi:<http://dx.doi.org/10.1016/j.cor.2006.04.003>. URL <http://www.sciencedirect.com/science/article/pii/S0305054806001213>. Part Special Issue: New Trends in Locational Analysis.
- Ramos, J.I. 2007. Piecewise-linearized methods for single degree-of-freedom problems. *Communications in Nonlinear Science and Numerical Simulation* **12**(6) 1005 – 1022. doi:<http://dx.doi.org/10.1016/j.cnsns.2005.09.003>. URL <http://www.sciencedirect.com/science/article/pii/S1007570405001449>.
- Razi, Nasuh, Mumtaz Karatas. 2016. A multi-objective model for locating search and rescue boats. *European Journal of Operational Research* –doi:<http://dx.doi.org/10.1016/j.ejor.2016.03.026>. URL <http://www.sciencedirect.com/science/article/pii/S0377221716301540>.
- Royset, J. O., H. Sato. 2010. Route optimization for multiple searchers. *Naval Research Logistics* **57**(8) 701–717.
- Senol, Yunus Emre, Yusuf Volkan Aydogdu, Bekir Sahin, Ibrahim Kilic. 2015. Fault tree analysis of chemical cargo contamination by using fuzzy approach. *Expert Systems with Applications* **42**(12) 5232 – 5244. doi:<http://dx.doi.org/10.1016/j.eswa.2015.02.027>. URL <http://www.sciencedirect.com/science/article/pii/S0957417415001347>.
- Shechter, Steven M., Farhad Ghassemi, Yasin Gocgun, Martin L. Puterman. 2015. Technical note—trading off quick versus slow actions in optimal search. *Operations Research* **63**(2) 353–362.
- Stone, Lawrence D., Johannes O. Royset, Alan R. Washburn. 2016. *Optimal Search for Moving Targets*. 1st ed. International Series in Operations Research & Management Science (Book 237), Springer.
- Suzuki, Atsuo, Zvi Drezner. 1996. The p-center location problem in an area. *Location Science* **4**(1–2) 69 – 82. doi:[http://dx.doi.org/10.1016/S0966-8349\(96\)00012-5](http://dx.doi.org/10.1016/S0966-8349(96)00012-5). URL <http://www.sciencedirect.com/science/article/pii/S0966834996000125>.
- Talley, Wayne K., Tsz Leung Yip, Di Jin. 2012. Determinants of vessel-accident bunker spills. *Transportation Research Part D: Transport and Environment* **17**(8) 605 – 609. doi:<http://dx.doi.org/10.1016/j.trd.2012.07.005>. URL <http://www.sciencedirect.com/science/article/pii/S1361920912000788>.
- Tavakoli, Asad, Constance Lightner. 2004. Implementing a mathematical model for locating {EMS} vehicles in fayetteville, {NC}. *Computers and Operations Research* **31**(9)

1549 – 1563. doi:[http://dx.doi.org/10.1016/S0305-0548\(03\)00108-4](http://dx.doi.org/10.1016/S0305-0548(03)00108-4). URL <http://www.sciencedirect.com/science/article/pii/S0305054803001084>.

Toro-Díaz, Hector, Maria E. Mayorga, Sunarin Chanta, Laura A. McLay. 2013. Joint location and dispatching decisions for emergency medical services. *Computers and Industrial Engineering* **64**(4) 917 – 928. doi:<http://dx.doi.org/10.1016/j.cie.2013.01.002>. URL <http://www.sciencedirect.com/science/article/pii/S0360835213000077>.

Vanem, Erik, Oyvind Endresen, Rolf Skjong. 2008. Cost-effectiveness criteria for marine oil spill preventive measures. *Reliability Engineering and System Safety* **93**(9) 1354 – 1368.

Viggo, Jean-Hansen. 2003. Skipstrafikken i området Lofoten - Barentshavet. *Transportøkonomisk institutt* (644/2003).

Wagner, Michael R., Zinovy Radovilsky. 2012. Optimizing boat resources at the u.s. coast guard: Deterministic and stochastic models. *Operations Research* **60**(5) 1035–1049. doi: 10.1287/opre.1120.1085. URL <http://dx.doi.org/10.1287/opre.1120.1085>.

Wang, Wenlin, Daniel E. Rivera, Karl G. Kempf. 2007. Model predictive control strategies for supply chain management in semiconductor manufacturing. *International Journal of Production Economics* **107**(1) 56 – 77.

White, I, F. Molloy. 2003. Factors that determine the cost of oil spills. *The International Tanker Owners Pollution Federation Limited*. London EC3A7AX, United Kingdom.

Wysokiński, Michał, Robert Marcjan, Jacek Dajda. 2014. Decision support software for search and rescue operations. *Procedia Computer Science* **35** 776 – 785. doi:<http://dx.doi.org/10.1016/j.procs.2014.08.160>. URL <http://www.sciencedirect.com/science/article/pii/S1877050914011259>. Knowledge-Based and Intelligent Information and Engineering Systems 18th Annual Conference, KES-2014 Gdynia, Poland, September 2014 Proceedings.

Zhang, Yue, Donald E. Brown. 2013. Police patrol districting method and simulation evaluation using agent-based model & gis. *Security Informatics* **2**(1) 1–13. doi:10.1186/2190-8532-2-7. URL <http://dx.doi.org/10.1186/2190-8532-2-7>.